Accepted Manuscript

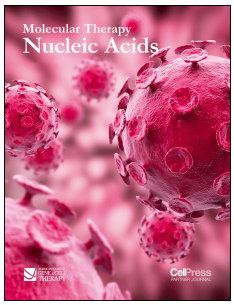

Targeting herpes simplex virus-1 gD by a DNA aptamer can be an effective new strategy to curb viral infection

Tejabhiram Yadavalli, Alex Agelidis, Dinesh Jaishankar, Kyle Mangano, Neel Thakkar, Kumar Penmetcha, Deepak Shukla

PII: S2162-2531(17)30270-6

DOI: 10.1016/j.omtn.2017.10.009

Reference: OMTN 154

To appear in: *Molecular Therapy: Nucleic Acid*

Received Date: 20 June 2017

Accepted Date: 14 October 2017

Please cite this article as: Yadavalli T, Agelidis A, Jaishankar D, Mangano K, Thakkar N, Penmetcha K, Shukla D, Targeting herpes simplex virus-1 gD by a DNA aptamer can be an effective new strategy to curb viral infection, *Molecular Therapy: Nucleic Acid* (2017), doi: 10.1016/j.omtn.2017.10.009.

1 **Targeting herpes simplex virus-1 gD by a DNA aptamer can be an effective new strategy to**
2 **curb viral infection**

3 Tejabhiram Yadavalli[1], Alex Agelidis[1, 2], Dinesh Jaishankar[1, 3], Kyle Mangano[4], Neel Thakkar[1],
4 Kumar Penmetcha[5], Deepak Shukla[1, 2, 3]*

5 [1]Department of Ophthalmology and Visual Sciences, University of Illinois at Chicago, IL 60612

6 [2]Department of Microbiology and Immunology, University of Illinois at Chicago, IL 60612

7 [3]Department of Bioengineering, University of Illinois at Chicago, IL 60607

8 [4]Medicinal Chemistry and Pharmacognosy, University of Illinois at Chicago, IL 60612

9 [5]Biomedical Research Institute, National Institute of Advanced Industrial Science and
10 Technology (AIST), Tsukuba Science City, Ibaraki 305-8566, Japan

11 *Corresponding Author: Correspondence should be addressed to D.S. (dshukla@uic.edu)

12 Research work was done in Chicago, Illinois, USA

13 Prof. Deepak Shukla, PhD

14 1855 West Taylor Street, Chicago, IL USA, email:dshukla@uic.edu, Phone: 312-355-0908

15

16 **Short Title**: *In vivo* targeting of HSV-1 gD by a DNA aptamer

17

18 **Abstract**

19 Herpes simplex virus type 1 (HSV-1) is an important factor for vision loss in developed
20 countries. A challenging aspect of the ocular infection by HSV-1 is that common treatments
21 such as acyclovir fail to provide effective topical remedies. Likewise, it is not very clear whether
22 the viral glycoproteins for entry can be targeted for an effective therapy against ocular herpes
23 *in vivo*. Here we demonstrate that HSV-1 envelope glycoprotein gD, which is essential for viral
24 entry and spread, can be specifically targeted by topical applications of a small DNA aptamer to
25 effectively control ocular infection by the virus. Our 45 nucleotide long DNA aptamer showed
26 high affinity for HSV-1 gD (Kd = 50 nM), which is strong enough to disrupt the binding of gD to
27 its cognate host receptors. Our studies showed significant restriction of viral entry and
28 replication both *in vitro* and e*x vivo* studies. *In vivo* experiments in mice also resulted in loss of
29 ocular infection under prophylactic treatment and statistically significant lower infection under
30 therapeutic modality compared to random DNA controls. Thus, our studies validate the
31 possibility that targeting HSV-1 entry glycoproteins such as gD can locally reduce the spread of
32 infection and define a novel DNA aptamer-based approach to control HSV-1 infection of the
33 eye.

34 **Introduction**

35 Herpes simplex virus type-1 (HSV-1), belonging to the family *Herpesviridae*, causes herpes
36 labialis and ocular keratitis which is one of the main causes of infectious blindness in the USA [1].
37 HSV-1 has a global sero-prevalence in the range of 60-90% with recurrent infections causing
38 corneal scarring, neovascularization and stromal keratitis [2,3]. HSV-1 might also lead to other
39 more serious diseases such as retinitis, encephalitis and sporadic cases of systemic morbidities,
40 especially among immunocompromised patients [4]. HSV-1 consists of a double stranded DNA
41 genome enclosed within an icosahedral capsid that is surrounded by a double layered lipid
42 membrane envelope[5]. The viral envelope is covered with a dozen different glycoproteins that
43 include four essential glycoproteins, namely gB, gD and gH/gL, which facilitate virus host
44 membrane fusion required for virus entry and cell-to-cell spread [6]. The glycoprotein gD is
45 essential for interaction with host receptors leading to viral entry and/or spread. It binds to cell
46 surface receptors nectin-1, HVEM and 3-*O* sulfated heparan sulfate with similar affinity and the
47 Kd values appear to be in low micromolar to higher nanomolar range [7]. Because gD is essential
48 for viral infectivity, is abundantly expressed on the HSV-1 envelope and the plasma membrane
49 of infected cells, and does not share homologies to any known host cell proteins, it can be an
50 ideal candidate for antiviral drug targeting.

51 Nucleic acid aptamers are single stranded oligonucleotides that provide unprecedented binding
52 specificity and equally strong affinity to a variety of targets including inorganic molecules,
53 cellular proteins and viral glycoproteins [8, 9, 10, 11]. Their sizes range from a few nucleotides (nt) to
54 a few hundred nts. Among many types of applications, medical or non-medical, aptamers can

55 also be used for target-based topical therapies for HSV-1 infection. Such alternative treatments
56 are crucial since conventional anti-HSV therapies such as acyclovir and other nucleoside analogs
57 cause serious side effects and are prone to the development of viral resistance [12]. Similar issues
58 exist with the treatment of HSV-1 infection of the eye, which can linger for months in many
59 cases and topical treatments fail to control the ocular disease manifestations. So far there have
60 been only two studies reporting the use of aptamers for neutralizing HSV infectivity. Our
61 collaborators reported the use of an RNA aptamer in cell cultures which targeted HSV-1 gD[13]
62 and Moore *et al.* reported the use of another RNA aptamer which targeted the gD protein of
63 HSV-2[14]. The original RNA aptamer developed by our collaborators was 113 nt long and highly
64 specific for HSV-1 gD as it did not block infection of HSV-2 virions[13].

65 Given their ability to acquire high degree of structural divergence and ease of selection against
66 any target of interest, RNA aptamers offer many advantages over newer technologies that
67 currently exist [8, 9, 10, 11]. However, two major disadvantages include lack of stability and higher
68 manufacturing costs, which can hinder commercialization efforts. DNA aptamers, on the other
69 hand, can be more stable, easier to manufacture and more cost effective. Therefore, in our
70 quest to study HSV-1 gD in viral entry and spread *in vivo* and also to develop an effective topical
71 therapy against ocular herpes, we designed and tested a DNA aptamer (DApt) that derives its
72 sequence from the mini-1 RNA aptamer used by our collaborators [13]. The DNA-based design of
73 this aptamer preserves the functional characteristics of the mini-1 RNA aptamer.[13] Here we
74 show the target specificity and antiviral efficacy of DApt using corneal cell cultures, corneal
75 organ cultures and mice models of ocular infection. To the best of our knowledge, ours is the
76 very first report demonstrating the effect of blocking gD on HSV-1 infectivity in the eye and the

77 use of DNA aptamers as viral entry blocking agents against HSV-1. It is also the most thorough
78 study using any kind of aptamer against herpesviruses.

79 **Results**

80 **Identification and structural characterization of DApt that binds to HSV-1 gD**

81 In order to study the significance of inhibiting gD on HSV-1 infectivity *in vivo* we designed and
82 tested the DNA version of an RNA aptamer that very specifically targets HSV-1 gD.[13] We
83 reasoned that a DNA aptamer, which preserves many features of the RNA aptamer, may
84 provide a more viable therapeutic option against HSV-1 infection. The sequence of DApt was
85 derived after mini-1 RNA aptamer, which contains the gD binding region of the original RNA
86 aptamer sequence[13]. The sequence for the short RNA aptamer that preserves most of the
87 antiviral activity of the parent RNA aptamer and its DNA replica are shown in figure 1a. The gD
88 binding ability of mini-1 RNA aptamer was already reported to be similar to the parent RNA
89 aptamer[13]. The secondary structures of the mini-1 RNA aptamer and DApt were predicted using
90 IDT OligoAnalyzer tool. The two sequences appear to preserve the loop structures that are
91 important for interaction with gD[13]. The distance between the loops provides sufficient
92 flexibility for the aptamers to conform to the receptor binding region of the surface exposed 3-
93 dimensional structure of gD [15]. Based on similar studies, the structural flexibility of DApt may be
94 slightly lower than its RNA homolog, which as shown below, did not affect its antiviral
95 properties against HSV-1 [16, 17]. The entropy values were predicted as -443.01 and -294 cal.K^{-1}
96 mol^{-1} for RNA and DApt, respectively. The latter suggests a higher thermostability and shelf life
97 for DApt.

98 **DApt binds specifically to HSV-1 gD**

99 DApt binding affinity towards gD protein was evaluated along with two control proteins. The
100 controls used included a cell surface gD receptor protein, nectin-1, and HSV-1 envelope
101 glycoprotein, gB. To verify the binding specificity, we conducted an immunofluorescence study
102 using FAM-tagged-DApt (Integrated DNA Technologies, USA) to assess its binding specificity [18].
103 Chinese Hamster Ovary (CHO) cells transfected with either Nectin-1, HSV-1 glycoproteins gD or
104 gB were permeabilized and incubated with FAM-DApt for a period of 30 minutes before
105 immunofluorescence imaging. Only the cells expressing gD viral protein had the presence of
106 FAM-aptamer compared to cells expressing empty vector (not shown), Nectin-1 or gB (figure
107 1b). This assay has a big advantage that it examines binding of a ligand (aptamer) against a cell
108 surface-expressed full-length protein, which is present in its native form. All other gD binding
109 assays use a purified but truncated form of gD, which may not be folded exactly as its
110 membrane bound native form. The binding specificity of the aptamer to gD protein was further
111 quantified via a modified SYBR Green (SG) assay [19]. As the intensity of SG varied based on the
112 availability of free aptamers (not bound to protein) in the solution, a nonlinear regression
113 analysis of the determined values was plotted to give specific binding affinity constant (Kd) of
114 53.92 nM (figure 1c). Taken together, these results indicate that DApt binds to glycoprotein gD
115 albeit with a lower affinity than its parent mini-1 RNA aptamer (4 nM).

116 **DApt is non-toxic and does not induce host response**

117 To rule out cytotoxicity of DApt, an MTT assay was performed. HCE cells were treated with the
118 indicated concentrations of DApt and a random DNA aptamer sequence (RDApt) was used as a

119 control. The results (figure 1d) showed no difference in cell viability at concentrations as high as
120 100 µM. Furthermore, RNA aptamers are known to generate elevated cytokine response in host
121 cells which in turn would inhibit viral replication [16, 17]. Hence, to understand the role of our
122 aptamer in influencing host cytokine response, HCEs were incubated with DApt and RDApt
123 aptamers in the absence of an infection. RNA collected from the samples was reverse
124 transcribed to DNA and evaluated for any change in regulatory cytokines such as IFN-α, IFN-β
125 and TNF-α. No significant change in cytokine levels was observed in cells exposed to either DApt
126 or the RDApt, when compared to the mock-treated cells (figure 1e). These results validate that
127 any antiviral activity shown by DApt would in fact be due to viral protein neutralization and not
128 due to changes in cytokine activity.

129 **DApt inhibits HSV-1 entry**

130 Since our aptamer binds gD with high affinity, we predicted that it has the ability to neutralize
131 infectious virions by disrupting interactions with the host receptor. Experiments were
132 conducted by incubating known concentrations of DApt with a β-galactosidase expressing HSV-
133 1 reporter virus (KOS gL86). DApt restricted viral entry by approximately 50% and 80% at
134 concentrations 2 µM and 32 µM respectively, when infected at an MOI of 10 (figure 2a).
135 Furthermore, immunoblotting of the HSV-1 (17-GFP) infected cell lysate for ICP0 (one of the
136 early viral gene products made immediately upon HSV-1 entry) showed significantly lower
137 levels in cells treated with DApt compared to RDApt (figures 2b-2c). Finally,
138 immunofluorescence imaging showed a significant reduction in entry of GFP-tagged HSV-1 (17-

139 GFP) into HCE cells treated with DApt (figure 2d). Collectively, these results indicate that DApt
140 inhibits HSV-1 entry.

141 **DApt reduces overall HSV-1 infection**

142 Since DApt blocks viral entry, it should reduce the number of virions entering into cells, which in
143 turn, should result in loss of viral infectivity. To test this, HCE cells were infected with HSV-
144 1(KOS) at MOI of 1 after they were neutralized with DApt/RDApt/Acyclovir at indicated
145 concentrations. At 24 hpi, cell lysates and cell supernatant (containing released virus) were
146 collected for immunoblotting and viral titer analysis respectively. We observed a decrease in
147 viral protein (gD) by approximately 50% and 70% at concentrations of 5 µM and 10 µM
148 respectively (figures 3a-3b). We also saw significantly lower released viral titers in these
149 samples (figure 3c). Similar experiments at varied MOI and lower aptamer concentrations were
150 conducted with similar results (figures S1a-S1b, figures S2a-S2b). To further understand if DApt
151 would have neutralizing properties against acyclovir resistant strains, similar experiments were
152 conducted using HSV-1 TK-12 strain, which is an acyclovir resistant strain because it lacks viral
153 thymidine kinase, the molecular target of acyclovir. We found that there was no significant
154 difference in the neutralizing ability of the aptamer between acyclovir sensitive or resistant
155 strain (figures S1c-S1d). In all cases, the aptamer showed similar virus neutralizing potential,
156 clearly suggesting that an aptamer-based therapy will work equally well against acyclovir
157 resistant strains.

158 **DApt restricts cell-to-cell fusion**

159 It is well known that after infection, HSV-1 spreads from one cell to another by enabling
160 membrane fusion to cause multinucleated syncytia formation, which requires gD and its
161 receptors [20]. Since DApt blocks gD with much higher affinity than gD's affinity for any of its
162 receptors [7], we hypothesized that DApt should have the ability to disrupt HSV-1-mediated
163 membrane fusion. The effect on membrane fusion was studied both visually and through a
164 luciferase based reporter assay described previously [21, 22], at the EC_{50} concentration of DApt.
165 Target cells expressing the entry receptor nectin-1 and luciferase gene were mixed with the
166 effector cells expressing viral glycoproteins and T7 RNA polymerase (figure 3d). Fusion was
167 monitored as a function of luciferase activity on its substrate (figure 3e) and in parallel
168 visualized by staining the cellular nuclei with DAPI stain (figure 3f). As hypothesized, fusion was
169 restricted to a significant extent (35%) by DApt compared to RDApt and mock-treated cells. This
170 indicates that DApt not only restricts extracellular entry of the virus but it can also block
171 intracellular spread by restricting fusion pore formation between neighboring cells, which could
172 be a mechanism behind the therapeutic effects of DApt against existing HSV-1 infections.

173 **DApt restricts spread and infection in *ex vivo* corneal model**

174 Based on the evidence gathered in the previous section, an *ex vivo* porcine corneal model was
175 developed to investigate the extent of viral spread in treated and untreated conditions. We and
176 others have demonstrated that cultured porcine corneas can provide an infection model that
177 mimics many key characteristics of human clinical disease [23,24]. Neutralization and therapeutic
178 studies were conducted using equal amounts of HSV-1 17-GFP virus to infect porcine corneal
179 epithelium. A schematic representing the process of porcine corneal tissue infection and

180 treatment is depicted in figure 4a. Neutralization was performed by incubating (pre-heated and
181 cooled) DApt with the virus for a period of 30 minutes before applying them onto the cornea.
182 The site of epithelial debridement (and infection) was closely monitored for a period of 72 h.
183 Stereoscopic images taken at 72 hpi were analyzed using ImageJ software to quantify the
184 extent of HSV-1 spread in the presence or absence of DApt neutralization. Based on the notion
185 that non-neutralized virus would constitute infection (radial spread of the virus), extent of viral
186 spread (GFP) was monitored for a period of 72 h in all three treatment groups. We observed
187 significantly lower infection (radial spread of GFP) in DApt treated corneas when compared to
188 RDApt and mock treated corneas (figures 4b-4c).

189 In a separate experiment, the therapeutic efficacy of DApt was evaluated by starting the
190 treatment at 48 h post epithelial debridement and infection with a GFP Virus (HSV-1 17 GFP).
191 DApt, RDApt or mock (PBS) treatments were applied as eye drops to the cornea every 24 hours
192 and the progression of infection was monitored by a Zeiss stereoscope. It was evident that
193 mock treated and RDApt treated corneas become rampant with infectious spread (green) while
194 very minute spread is observed in the DApt treated corneas (figure 4d). Although viral (green)
195 spread was observed in DApt treated corneas, it was significantly lower when compared to its
196 counterparts (figure 4e).

197 To understand whether the discontinuation of DApt treatment would lead to an increase in
198 viral spread, 7 dpi, one set of corneas (previously treated with DApt) were left untreated for 72
199 h while the other sets were continued on DApt treatment. As expected, we saw an increase in

200 viral spread in the treatment discontinued cornea compared to the treated ones (figures 4f-4g),
201 indicating that DApt was able to continuously restrict viral spread during this time frame.

202 **DApt reduces infectious spread of HSV-1 *in vivo* corneal models**

203 Based on the results we observed in the *ex vivo* models, we tested the prophylactic and
204 neutralization ability of DApt to suppress HSV-1 infection in an intact animal (mouse) model
205 (figure 5a). Post epithelial debridement, mice eyes were treated with either DApt or RDApt
206 according to prophylaxis or neutralization protocols prior to infection with HSV-1 17-GFP. We
207 used a high virus titer ($2x10^7$ PFU) for these experiments to study the effect of DApt on viral
208 entry at earlier time points. Representative stereoscope images taken at 48 hpi show that
209 corneas treated with DApt had lower infection (green spots) than those treated with RDApt
210 (figure 5b). Tear samples collected from the mice eyes at 72 hpi were assayed to quantify the
211 viral titers. In both prophylactic and neutralization treatments, we observed lower viral titers in
212 the eye swabs of mice treated with DApt compared to RDApt (figure 5c). Moreover,
213 quantitative PCR analysis of mRNA extracted from mouse corneal tissue showed significant
214 reductions in the viral gD transcripts for prophylaxis (80% reduction) and neutralization (50%
215 reduction) DApt treatments (figures 5d-5e). An interesting observation to note is the difference
216 in infectivity between the prophylaxis and neutralization models. We observed more infection
217 in the prophylaxis model compared to the neutralization model. This difference may be
218 attributed to the experimental design. While in the prophylaxis model the eyes are first pre-
219 treated with the treatments for 30 mins and then infected, in the neutralization model, the
220 virus and the treatments are mixed together for 30 mins and then added to the eye. The

221 process of mixing the aptamers with the virus might have resulted in non-specific binding
222 between the negatively charged RDApt and virus resulting in lower rates of infection compared
223 to the prophylaxis model.

224 We also evaluated for cellular cytokine transcripts such as IFN-α, IFN-β and IL-1β, which are
225 normally induced upon infection. qRT-PCR analysis revealed that DApt significantly reduced the
226 induction of cytokine transcripts compared to RDApt only in the prophylaxis model whereas no
227 change was observed in the induction of the cytokine transcripts between the DApt and RDApt
228 treated cells in the neutralization model possibly because of the experimental design
229 mentioned above (figures 5d-5e).

230 Since HSV-1 mostly spreads via cell-to-cell in corneal tissues and uses gD for this process, we
231 wanted to test the therapeutic ability of DApt to specifically bind to gD and block HSV-1
232 infection. DApt or RDApt were topically applied to infected murine corneas at 24 hours post
233 epithelial debridement and infection (figure 6a). A 10-fold lower virus titer ($2x10^6$ PFU) was
234 used in the therapeutic model to study the effect of DApt treatment at later stages of viral
235 infection (post entry) for a longer period of time (14 days). Representative stereoscope images
236 taken 3 days post infection show that mice in both treatment groups were infected albeit DApt
237 treatment group had a slightly lower amount of infection (figure 6b). To further assess
238 infection, tear samples collected from the mice eyes were assayed to titer the presence of
239 virus. Interestingly, while no differences in virus titers were observed on day 4, significant
240 reduction of virus titers was observed on day 7 (figure 6c). We are not sure why we do not see
241 changes on day 4, however the low viral titers seen during these experiments could be

242 attributed to non-specific-charge based neutralization, similar to those described above, by
243 RDApt during our therapeutic treatment. We also monitored corneal disease progression by
244 recording scores assessed by a blind observer. The DApt treated mice consistently showed
245 lower clinical scores compared to the RDApt treated group and were significant at 7 and 10 dpi
246 (figure 6d). Quantitative PCR analysis of mRNA extracted from excised corneas at 14 dpi
247 showed 45% lower viral gD transcripts with DApt treatment compared to RDApt treatment
248 (figure 6e). The IFN-α, IFN-β and IL-1β response was also significantly lower with DApt
249 treatment than with RDApt (figure 6e). This could be attributed to the presence of lower
250 infection in those treated with DApt as opposed to RDApt. These results correspond well with
251 the cytokine levels recorded for the prophylaxis treatments (figure 5d). Collectively, using a
252 variety of treatment regimens *in vivo*, our findings suggest that DApt can effectively block HSV-
253 1 viral infection and spread in the cornea, and together our findings provide promise for future
254 use of DApt in clinical settings.

255 **Discussion**

256 Only two aptamers have been superficially tested for efficacy against HSV in the past and both
257 aptamers were RNA in composition [13, 14]. Although RNA aptamers generally have a more
258 versatile structure enabling them to form multiple secondary structures [25], their stability in
259 biological systems is low and is further compounded by a high degradation rate at room
260 temperature or higher. Multiple stabilization methods have been proposed for RNA [26], however
261 they have shown to weaken their ability to bind to desired targets and also to negatively impact
262 cost effectiveness. DNA is a comparatively stable molecule with respect to biological systems [27]

263 although its versatility is not considered equivalent to RNA. In this work, a DApt was designed
264 based on the mini-1 RNA aptamer, which is already shown to bind HSV-1 gD with very strong
265 affinity by Gopinath et al.[13] To our surprise, the shorter DNA preserves key structural features
266 of its native RNA form and most significantly, it binds gD albeit with lower affinity than the
267 parent RNA aptamer. Our serendipity with DApt was observed when we used the DNA clone as
268 a control for testing the antiviral activity of the parent RNA aptamer (figure S2c). To our
269 surprise, the DNA form had good stability and high anti-HSV-1 activity in *ex vivo* models.
270 Furthermore, the cost of the DNA form was 10 fold cheaper than its RNA parent. Although
271 preliminary experiments (figure S2c) with the parent RNA aptamer were conducted, this study
272 was geared towards understanding the efficacy of DApt in controlling HSV-1 infection. Overall,
273 our experiments suggest that DApt can provide a suitable alternative to many conventional
274 designs and provide an effective strategy for viral glycoprotein-targeting drug discovery efforts.

275 The results obtained from the viral entry assay show 50-80% reduction in viral entry through
276 neutralization of the virus by DApt with an EC_{50} of 2 µM, as opposed to RDApt (figure 2). The 24
277 h viral replication study showed similar results, reiterating the role of DApt in reducing initial
278 viral entry corresponding to lower infectious spread (figures 3a-3c). Furthermore, the ability of
279 DApt to inhibit cell fusion signifies that this aptamer has a multifaceted role in not only reducing
280 initial viral entry but also restricting intracellular viral spread via blocking syncytia formation
281 (figures 3d-3f).The DApt did not cause any toxic effects and did not induce any unusual cytokine
282 responses suggesting that the antiviral activity of DApt was through specifically binding to gD
283 (figures 1d-1e). . HSV-1 gD protein interacts with host membrane receptors, HVEM and Nectin-
284 1, to facilitate entry into cells. While the affinity of interactions between gD and HVEM/Nectin-1

285 is in low micro molar range, it has been shown that the binding affinity of a interfering molecule
286 to effectively disrupt HVEM/Nectin-1-gD interactions needs to be in the nanomolar range (40
287 nM)[13]. Our *in-silico* results have shown that the binding affinity of DApt is also in the
288 comparable range (50 nM), which is strong enough to competitively interfere with gD/receptor
289 interactions. It is also important to note that while the IDT Oligo-analyzer tool suggests
290 similarities in structural characteristics between DApt and its parent mini-1 RNA aptamer, many
291 other differences including inhibitory effects due to charged nature of the oligomers causing a
292 "heparin" like effect may influence the virus inhibitory properties of the aptamer. All of which
293 will be thoroughly analyzed in our future studies that will also map out the binding sites of the
294 aptamer on gD crystal structure.

295 An interesting aspect of using aptamers in therapy is that aptamer binding affinities change
296 with variations in salt content, pH and temperature.[28, 29] While examining this possibility with
297 our treatment we noted that during *in vitro* experiments when DApt was compared to Acyclovir
298 or TFT (Trifluorothymidine) the therapeutic effects of the aptamer were not as strong,
299 especially when the treatments were started 2 hpi for a period of 24 hours (figure S3a). To
300 understand this anomaly further, we performed neutralization experiments using aptamers
301 dissolved in different buffers. As suspected, DApt had no virus neutralizing ability when the salt
302 concentration in buffers was changed, which may be a limitation of our approach. However, as
303 discussed below, to our satisfaction our original aptamer formulation in PBS showed excellent
304 results in ex vivo cornea cultures and murine ocular infections. When DApt was tested for its
305 efficacy in restricting viral entry in porcine corneal tissue cultures infected with GFP-tagged

306 HSV-1 (17-GFP) it was clear that viruses neutralized with DApt showed lower radial spread
307 compared to mock or RDApt treatments (figure 5).

308 Similar therapeutic effects were seen when the aptamer was applied as a topical eye drop over
309 porcine corneal tissues post HSV-1 infection (figure 4). Noticeably, the infectious spread of the
310 GFP virus was contained throughout the treatment period and regained when the treatment
311 was stopped. This could be because DApt is able to restrict newly produced viral particles from
312 entering nearby uninfected cells while also restricting cell-to-cell fusion and thereby inhibiting
313 intracellular viral spread. Also, the pH and salt concentrations of the excised cornea might
314 actually be complementing the DApt's neutralization ability, which were lacking in the *in vitro*
315 culture model. Mock and RDApt treated samples were observed to have dendritic lesions
316 continue to form over a period of 10 days. However, the limitation of the aptamer treatment
317 was that it was not able to completely eliminate the presence of the virus from the corneal
318 tissue.

319 To further test the efficacy of DApt in *in vivo* models, mouse corneal tissue was infected with
320 GFP virus pre-treated either prophylactically or through neutralization (figure 5). The studies
321 showed protective ability of DApt in restricting viral entry and spread in corneal tissue when
322 applied prophylactically. Mice pre-infected and then treated with DApt showed lower disease
323 scores, viral titters and viral RNA transcripts suggesting its role in reducing HSV-1 infection *in*
324 *vivo*. However the results obtained in the *in vivo* therapeutic model were not as prominent as
325 the *ex vivo* therapeutic model or *in vivo* prophylactic model we conducted. This could be
326 attributed to lower retention time or change in aptamer concentration on the corneal surface

327 *in vivo* compared to *ex vivo* corneas and the extent of viral spread to the deeper layers of the
328 cornea during *in vivo* infection. We believe that while our DApt is an excellent entry inhibitor
329 that shows potential prophylactic therapy against HSV-1 infection, further improvements
330 involving extended retention/release models would make it an attractive candidate as a
331 therapeutic against ocular herpes infection.

332 In conclusion, this is the first study to show a comprehensive decrease in HSV-1 infection using
333 a DNA aptamer. The 45 nucleotide DApt was found to bind to HSV-1 surface glycoprotein gD
334 and was able to restrict viral entry into host cells. Its role in inhibiting cell-to-cell fusion and
335 consequently restricting viral spread was also established in this study. Furthermore, its role as
336 a therapeutic agent was investigated using both *ex vivo* and *in vivo* models. While DApt shows
337 significant therapeutic efficacy *in vivo*, our results suggest that as an entry inhibitor it would be
338 able to show greater efficacy when used synergistically with other topical therapeutics such as
339 TFT, ganciclovir or inhibitors of heparanase that can reduce viral release and resultant
340 pathogenesis[30, 31]. These studies will be part of our future work, which will also include studies
341 directed towards determining the structural differences between the DNA and RNA aptamers
342 and mapping out the aptamer binding sites on gD. Future studies will also shed more light on
343 the clinical applicability of our aptamer.

344 **Materials and Methods**

345 **Cells, Virus, Media and Plasmids**

346 Human Corneal Epithelial cells (RCB1834 HCE-T) was obtained from Kozaburo Hayashi (National
347 Eye Institute, Bethesda, MD) and was cultured in MEM (Life Technologies, Carlsbad, CA) with

348 10% fetal bovine serum (FBS, Sigma-Aldrich, St. Louis, MO) and 1% penicillin/streptomycin (P/S,
349 Life Technologies). The African green monkey kidney (VERO) cell lines were obtained from Dr.
350 Patricia G. Spear (Northwestern University, Chicago, IL) and cultured in DMEM (Life
351 Technologies) with 10% FBS and 1% P/S. Chinese hamster ovary (CHO-K1) cells were provided
352 by P.G. Spear (Northwestern University). CHO-K1 cells were passaged in Ham's F12 medium
353 (Gibco/BRL, Carlsbad, CA, USA) supplemented with 10% fetal bovine serum (FBS) and penicillin
354 and streptomycin (P/S) (Sigma).

355 All the oligo sequences, including DApt, RDApt, RNA Aptamer and FAM Tagged DApt, were
356 purchased from IDT (Integrated DNA Technologies). Aptamers were used as received and
357 dissolved in PBS (DApt/RDApt) or Tris-HCl (RNA Aptamer) and stored at -20 °C. Aliquots of 100
358 µL aptamers were heated to 95 °C for 3 minutes cooled on ice prior to use in any experiments.
359 Trifluorothymidine (TFT) and acyclovir (ACV) were purchased from Selleckchem, and stock
360 solutions were prepared in DMSO and stored at -20 °C.

361 Three strains of HSV-1 were used: wild type HSV-1 KOS; β-galactosidase expressing HSV-1
362 reporter virus (gL86); Green Fluorescence Protein-tagged HSV-1 17-GFP (purified using sucrose
363 gradient). Minimum essential medium (MEM; Gibco) and OptiMEM (Gibco) were used in the 6
364 h and 24 h infection models. Dulbecco's minimum essential medium (Gibco) mixed with 5%
365 methyl cellulose (Sigma Aldrich) was used for obtaining plaque assays. Plasmids for gB, gD, gH,
366 gL, Luciferase gene, T7 promoter sequence plasmids (synthesized by standardized protocols
367 (Promega)), F12 media (Gibco) were used in cell-to-cell fusion assay. Soluble gB, gD and nectin-

368 1 proteins were kindly provided by G. H. Cohan (University of Pennsylvania, PA) and R. J.
369 Eisenberg (University of Pennsylvania, PA).

370 **SYBR Green Assay**

371 This assay is based on the ability of SYBR Green (SG, N',N'-dimethyl-N-[4-[(E)-(3-methyl-1,3-
372 benzothiazol-2-ylidene)methyl]-1-phenylquinolin-1-ium-2-yl]-N-propylpropane-1,3-diamine) to
373 fluoresce in the presence of a double stranded DNA molecule as an intercalation dye [19]. Briefly,
374 50 µL of multiple concentrations (200 nM to 1 nM) of soluble gD, gB and nectin-1 protein were
375 dispensed into a 96 well plate. DApt (4 µL) was added to each well and the samples were
376 incubated for a period of 30 minutes before 4 µL of SG was added to each well. DApt with SG,
377 DApt alone and SG alone were used as controls for the reaction. The fluorescence recorded at
378 520 nm was used to calculate binding affinity using the equation (1).

$$Affinity = \frac{f0 - f1}{f0}$$

379 Where f_0 is the fluorescence intensity of SG and DApt in the absence of any protein, while f1 is
380 the fluorescence emitted by SG and DApt in the presence of protein. As this equation would
381 give us the total amount of aptamer bound to the protein, a non-linear regression analysis of
382 the determined values was generated to calculate the binding affinity constant (Kd) for DApt.
383 GraphPad Prism software was used to generate the Kd values using triplicates of the
384 experiment.

385 **FAM-Tagged DApt Assay**

386 CHO cells (plated on glass bottomed dishes) were transfected with either a control plasmid
387 (empty vector), Nectin-1 plasmid, gB plasmid or gD plasmid (1.0 µg/mL) using standard
388 lipofectamine protocols and incubated for a period of 24 hours at 37°C at 5% CO_2. The cells
389 were then permeabilized with 4% PFA (Paraformaldehyde; Electron Microscopy Sciences, PA,
390 USA) for 30 minutes and stained with DAPI (NucBlue, Molecular Probes, USA) for 10 minutes.
391 Preheated and cooled 2 µM FAM-tagged-DApt (purchased from IDT) was then added to the
392 CHO cells and incubated for a period of 30 minutes before they were washed twice with PBS.
393 The cells were imaged at 63x on a laser Confocal Microscope (Leica, SP2) using z-stack full
394 image projection.

395 **MTT Cytotoxicity Assay**

396 DApt and RDApt oligonucleotides were tested for their toxicity by evaluating cellular
397 mitochondrial activity 24 hours post exposure. Briefly, HCE cells were plated in a 96 well plate
398 at a seeding density of $2x10^4$ per well and left overnight until they were 80% confluent. Various
399 concentrations of pre-heated (and cooled) DApt, RDApt and PBS were added to each well and
400 were allowed to incubate for a period of 24 h at 37 °C and 5% CO_2. Post incubation, wells were
401 washed with PBS twice before 100 µL of 0.5mg/mL MTT (3-(4,5-dimethylthiazol-2-yl)-2,5-
402 diphenyltetrazolium bromide) was added to each well and incubated for 4 hours. Formazan
403 crystals formed due to the mitochondrial activity were dissolved using acidified isopropanol
404 (0.1% HCl in isopropanol) and transferred to a new 96 well plate. The color developed was
405 analyzed by a Tecan GENios Pro microplate reader at 562 nm. Experiments were conducted in
406 triplicates and individually repeated 5 times.

407 **Quantitative PCR**

408 This protocol was used to extract cellular RNA and quantify cellular transcript levels, specifically
409 GAPDH, IFN-α, IFN-β and IL-1β. Viral gD RNA transcripts were also quantified using this method
410 in order to evaluate total infection in HCE cells and mouse corneal tissues. The process is similar
411 to those described in our previous reports [32] where RNA was extracted from cells using TRIzol
412 (Life Technologies) according to the manufacturer's protocol. RNA was then transcribed to
413 cDNA using High Capacity cDNA Reverse Transcription Kit (Applied Biosystems, Foster City, CA).
414 Real time quantitative PCR was performed with Fast SYBR Green Master Mix (Applied
415 Biosystems) using QuantStudio 7 Flex (Applied Biosystems). The primers used in this study are
416 listed in tables 1 and 2.

417 **Virus Neutralization by Aptamers**

418 Neutralization experiments was performed by adding required amount virus and pre-heated
419 and cooled DApt or RDApt in 400 µL OptiMEM followed by incubation for 30 minutes with
420 constant agitation at room temperature. At the end of 30 minutes, the mixture of the virus and
421 DApt were added to cells. 30 minutes neutralization allows for attaining adsorption equilibrium
422 between the aptamers and virus glycoproteins. PBS was added to the virus solution and
423 incubated for 30 minutes in the mock treated samples.

424 **Viral Entry Assay**

425 The viral entry assay was performed using protocols previously established [22]. HCEs were plated
426 at a seeding density of $2x10^4$ per well in a 96 well plate and were left overnight until they were

427 90% confluent. 0.1 µL/well (MOI 10) of gL86 virus ($2x10^8$ PFU/mL stock) solution was
428 neutralized either by PBS, RNA Aptamer, DApt or RDApt before they were added onto the
429 monolayer of cells. 6 h post infection, the wells were cleaned twice with PBS before the 100 µL
430 of β-galactosidase substrate (0.5% Nonidet P40 and 3 mg/mL ONPG, o-nitro-phenyl- β-d-
431 galactopyranoside; ImmunoPure, PIERCE, Rockford, IL) solution was added to each well. The
432 plates were stored at 37 °C for a period of 2 hours before the enzymatic activity was analyzed
433 using a GENESIS Pro Plate reader at 410 nm.

434 Viral entry assay was also evaluated through immunoblotting for HSV-1 ICP-0, an early gene
435 product made immediate upon viral entry. HCEs were plated at a seeding density of 1.2×10^6
436 per well in a 6 well plate and used when the cells reached 80% confluency. HSV-1 (KOS) at an
437 MOI of 10 was neutralized by either PBS/DApt/RDApt for a period of 30 minutes at the EC-50
438 concentration (2 µM) determined by β-galactosidase assay mentioned above. Cells were
439 infected for a period of 2 hours before fresh media was added to the cells. At 6 hpi, cells were
440 collected, lysed and immunoblotted for HSV-1 ICP0 protein and quantified using Image J
441 software.

442 **Viral Replication Assay**

443 HCEs were plated at a seeding density of 1.2×10^6 per well in a 6 well plate. Neutralization was
444 performed by incubating ACV/DApt/RDApt/Mock (at indicated concentrations) with HSV-1 KOS
445 (or TK-12) virus (0.6 µL of $2x10^8$ PFU/mL stock) for a period of 30 minutes before they were
446 added to the cell monolayer. At 2hpi cells were washed with PBS, replenished with MEM and

447 were incubated overnight for 24 hours before the cells were lysed and immunoblotted for HSV-
448 1 gD.

449 **Flow Cytometry**

450 HCEs were plated at a seeding density of 2 x 10^5 per well in a 24 well plate. HSV-1 17-GFP virus
451 (0.1 MOI) neutralization was performed by incubating either by DApt/RDApt for a period of 30
452 minutes at indicated concentrations (0 - 10 µM). Post neutralization, virus/Aptamer solution
453 was added to the cell monolayer and incubated at 37 °C at 5% CO_2 for 2 hours. Subsequently,
454 cells were washed with PBS twice and fresh MEM media was added to the cells. At 24 hpi, cells
455 were washed carefully with PBS and imaged with a stereoscope under the GFP channel prior to
456 preparing the cells for flow cytometry. Cells were then dislodged by adding 100 µL of trypsin to
457 each well for a period of 10 minutes and washed with PBS twice through centrifugation at 4000
458 rpm at 4 °C. Cell pellet was washed once FACS buffer (PBS with 2% FBS) before they were
459 suspended in 300 µL of FACS buffer. Cells were analyzed using a BD Accuri C6 plus instrument
460 under the live/singlet gates with 25,000 events per sample. All experiments were done in
461 quadruplicates.

462 **Immunofluorescence Imaging**

463 In order to visualize the virus restricting capabilities of DApt, HCEs were plated at a low seeding
464 density (1.2x10^5 cells/well) in glass bottom imaging dishes (MatTek Corporation, Ashland, MA,
465 USA). Neutralization treatment using 10 µM DApt was performed at high MOI (10) and the virus
466 solution was added to the cells and incubated at 4 °C for a period of 2 h to allow viral
467 adsorption. Entry was initiated by incubating the plate at 37°C for 30 minutes. The cells were

468 fixed in 4% paraformaldehyde (Electron Microscopy Sciences, Hatfield, PA, USA), permeabilized
469 with 0.01% Triton-X (Thermo Fisher Scientific), and stained with 4',6-diamidino-2-phenylindole
470 (DAPI; Life Technologies) to stain the nucleus. The images were captured under 63x objectives
471 using an observer microscope (Carl Zeiss Microscopy GmbH, Jena, Germany) with a spinning
472 disk (CSU-X1; Yokogawa, Tokyo, Japan).

473 **Immunoblotting**

474 Virally infected cell lysates were denatured in NuPAGE LDS Sample Buffer (Invitrogen, NP00007)
475 and heated to 80 °C for 10 min. Equal amounts of protein were added to 4–12% SDS–PAGE gel
476 and transferred to a nitrocellulose membrane. Nitrocellulose membrane was blocked in 5%
477 nonfat milk in tris-buffered saline (TBS) for 2 h at room temperature. After the nonspecific
478 binding blocking step was complete, membranes were incubated with primary antibodies
479 (mouse anti-ICP0 for 6 h infection model; mouse anti-gD monoclonal antibody (Ab-cam) for 24
480 h infection model) at dilutions of 1:1000 overnight at 4 °C. The following day the blots were
481 washed multiple times with 0.1% TTBS (0.1% Tween 20 in TBS) before the addition of
482 horseradish peroxidase conjugated anti-mouse IgG at dilutions of 1:25000 at room
483 temperature. Protein bands were visualized on an ImageQuant LAS 4000 imager (GE Healthcare
484 Life Sciences) after the addition of SuperSignal West Pico maximum sensitivity substrate
485 (Pierce, 34080). The density of the bands were quantified using ImageQuant TL image analysis
486 software (version:7). GAPDH was measured as a loading control.

487 **Cell-to-Cell Fusion Assay**

488 A standard virus free cell-to-cell fusion assay was performed as described previously [21]. Two
489 populations of CHO-K1 cells, designated target cells and effector cells, were generated. While
490 the target cell population was transfected with nectin-1 (1.0 µg) and plasmid expressing the
491 luciferase gene (0.5 µg), the effector cell population was transfected with HSV-1 glycoproteins
492 gB, gD, gH, and gL and T7 RNA polymerase (0.5 µg each in 6 well plates). Effector cells without
493 gB plasmid were used as a negative control as they would not contribute to active cell-to-cell
494 fusion. After transfection, effector and target cells were mixed in a 1:1 ratio and co-cultured in
495 24 well plates. PBS, DApt or RDApt at a final concentration of 2 µM was added to these
496 mixtures. Luciferase gene expression resulting from fusion of target and effector cells, 24 h post
497 mixing, was measured using a reporter lysis assay (Promega). All the experiments were
498 performed in triplicates and the plates were imaged to observe syncytia formation using a live
499 cell nucleus stain (Molecular probes NucBlu; R37605) at 10x magnification.

500 ***Ex vivo* porcine Corneal Infection Model**

501 Freshly sacrificed pig eyes were collected from a local butcher shop and were used no later
502 than 24 h. Two needle pokes were presented on each cornea using a 25 mm 30 gauge needle
503 (BD Precisionglide™) before the cornea was carved from the eye using a surgical blade. The
504 corneas were cleaned multiple times in PBS mixed with 5% Antifungal Antibacterial (Gibco)
505 solution before they were placed in a 12 well plate.

506 Neutralization treatment was performed by incubating DApt, RDApt or Mock (PBS) (final
507 concentration 10 µM) with $5x10^6$ PFU HSV-1 17-GFP virus. 30 minutes post incubation, the
508 solution was added to each cornea and left to infect for a period of 24 hours in cornea media

509 (MEM with 5% Antifungal Antibacterial and 1% insulin transferrin (Sigma)). 24 h later, the
510 corneas were washed with PBS twice and the media was replenished. Corneas were washed
511 and imaged every 24 hours for a period of 3 days. Quantification of the porcine corneal
512 infection in case of Neutralization studies was done using Image J software. The brightness and
513 contrast of the images was maintained constant and the threshold option was used to select
514 only the infectious zones. Once selected, the area of the selected zones was combined and
515 calculated to represent pixel counts.

516 Therapeutic treatment was initiated 48 h post infection of the corneas with $5x10^6$ PFU HSV-1
517 17-GFP virus. All the corneas were washed with PBS and imaged using Zeiss SteREO
518 Discovery.V20 at a constant exposure time of 400 ms at a magnification of 7.5X for the
519 presence of GFP virus. Triplicates of corneas were either treated with PBS, DApt or RDApt by
520 adding 100 µL of 10µM DApt onto the corneal poke site followed by addition of cornea media
521 (400 µL). The treatment was repeated every 24 h for a period of 10 days and images of the
522 cornea were collected subsequently before the addition of treatment solutions.

523 To understand if stopping DApt treatment would increase viral infection, 7 days post initial
524 infection, DApt treatment was stopped in one set of corneas while it was continued in another
525 set. The spread of virus was monitored by imaging both the set of corneas every 24 hours for
526 period of 3 days. At the end of 10 days, the corneas were discarded after the addition of 10%
527 bleach solution to each cornea.

528 **Mouse Cornea Infection**

529 Six to eight week old male and female BALB/c mice obtained from Charles River Laboratories
530 (Wilmington, MA) were housed at the University of Illinois at Chicago Animal Facility and used
531 for all animal experiments. Mice were anesthetized using ketamine (100 mg/kg) and xylazine (5
532 mg/kg) prior to the application of proparacaine hydrochloride ophthalmic solution, (Alcon
533 Laboratories, Inc., Texas, USA) and epithelial debridement of the right eye with a 30-G sterile
534 needle in a 3 × 3 grid pattern, as previously reported [33]. The level of anesthesia was determined
535 by loss of toe pinch/pedal withdrawal. Animals were maintained under a heat lamp until they
536 recovered from anesthesia. 1 µL of 10 µM DApt/RDApt/PBS was either used to neutralize HSV-1
537 17-GFP virus ($2x10^7$ PFU) or applied directly onto the cornea (prophylaxis) for 30 minutes. The
538 virus solution was then added onto the cornea to initiate infection. Mice were monitored every
539 24 h and imaged every 48 h for a period of 10 days to record any changes occurring due to
540 infection. Tear samples were collected using a calcium alginate tipped Calgiswab® dipped in 1
541 mL DMEM media which were swabbed on and around the eye 3 times to collect replicating
542 virus from the cornea. Animals were observed daily for complications and their weights were
543 monitored closely. Mice demonstrating pain or suffering were euthanized. Before euthanasia,
544 mice were injected intraperitoneally with a cocktail of Ketamine (100 mg/kg), and Xylazine (5
545 mg/kg) via intraperitoneal injection, and were cervically dislocated. This method is consistent
546 with the recommendations of the Panel on Euthanasia of the American Veterinary Medical
547 Association. Ten mice (5 male; 5 female) per treatment group were used for the experiment

548 To evaluate the therapeutic efficacy of DApt in *in vivo* animal model, mice were anesthetized as
549 described above and their right eyes were subjected to epithelial debridement prior to the
550 application of HSV-1 17-GFP virus ($2x10^6$ PFU). The mice were left untreated for a period of 24 h

551 before 5 µL of 10 µM DApt/RDApt/PBS was added to their eyes. Mice were imaged every 24 h
552 until 72 hours using Zeiss SteREO Discovery.V20 at a constant exposure time of 400 ms to check
553 for the presence of GFP virus. Ten mice (5 male; 5 female) per treatment group were used for
554 the experiment.

555 **Statistical Methods:**

556 All the statistical analysis conducted in the manuscript was performed using GraphPad Prism
557 Software Version-6. All the error bars represent Mean ± Standard Deviation (SD) which were
558 automatically calculated by the software. All one-way ANOVA analysis used Dunnett's multiple
559 comparison tests with a single pooled variance. All two-way ANOVA analysis used Sidak's
560 multiple comparison tests. Plaque numbers from the in vivo corneal swab were analyzed using
561 unpaired t-tests.

562 **Ethics Statement**

563 Animal care and procedures were performed in accordance with institutional and NIH
564 guidelines, and approved by the Animal Care Committee at University of Illinois at Chicago.
565 Biologic Resources Laboratory of the University of Illinois at Chicago has a modern animal
566 facility with several veterinarians on staff available for expert veterinary care and advice during
567 the project. The Animal Care Committee (ACC), at the University of Illinois at Chicago, approved
568 animal experiments under the permit no. ACC15-091

569 **Author Contributions**

570 T.Y., A.A., D.J., K.M. and N.T. conducted the experiments; T.Y., P.K. and D.S. designed the
571 experiments. T.Y, D.J, A.A and D.S wrote the paper.

572 **Acknowledgements**

573 The project was funded by a NIH grant (RO1 EY024710) to D. Shukla. Alex Agelidis was
574 supported by a NIH fellowship (F30 EY025981).

575 References

576 1. Coleman JL, Shukla D (2013) Recent advances in vaccine development for herpes simplex
577 virus types i and II. *Hum. Vaccines Immunother.;* **9:** 729-735

578 2. Shah A, Farooq AV, Tiwari V, Kim M-, Shukla D (2010) HSV-1 infection of human corneal
579 epithelial cells: Receptormediated entry and trends of re-infection. *Mol. Vision;* **16:** 2476-2486

580 3. Park PJ, Chang M, Garg N, Zhu J, Chang J-, Shukla D (2015) Corneal lymphangiogenesis in
581 herpetic stromal keratitis. *Surv. Ophthalmol.;* **60:** 60-71

582 4. Farooq, A. V., Shah, A., and Shukla, D. (2010) *The Role of Herpesviruses in Ocular Infections*,
583 pp. 115-123

584 5. Karasneh GA, Shukla D (2011) Herpes simplex virus infects most cell types in vitro: Clues to its
585 success. *Virol. J.;* **8:**

586 6. Hadigal S, Shukla D (2013) Exploiting herpes simplex virus entry for novel therapeutics.
587 *Viruses;* **5:** 1447-1465

588 7. Spear PG, Eisenberg RJ, Cohen GH (2000) Three Classes of Cell Surface Receptors for
589 Alphaherpesvirus Entry. *Virology;* **275:** 1-8

590 8. Bumcrot D, Manoharan M, Koteliansky V, Sah DWY (2006) RNAi therapeutics: A potential
591 new class of pharmaceutical drugs. *Nat. Chem. Biol.;* **2:** 711-719

592 9. Byrne JD, Betancourt T, Brannon-Peppas L (2008) Active targeting schemes for nanoparticle
593 systems in cancer therapeutics. *Adv. Drug Deliv. Rev.;* **60:** 1615-1626

594 10. **Nimjee, S. M., Rusconi, C. P., and Sullenger, B. A.** (2005) *Aptamers: An Emerging Class of*
595 *Therapeutics*, pp. 555-583

596 11. Tombelli S, Minunni M, Mascini M (2005) Analytical applications of aptamers. *Biosens.*
597 *Bioelectron.;* **20:** 2424-2434

598 12. Jiang Y-, Feng H, Lin Y-, Guo X- (2016) New strategies against drug resistance to herpes
599 simplex virus. *International Journal of Oral Science;* **8:** 1-6

600 13. Gopinath SCB, Hayashi K, Kumar PKR (2012) Aptamer that binds to the gD protein of herpes
601 simplex virus 1 and efficiently inhibits viral entry. *J. Virol.;* **86:** 6732-6744

602 14. Moore MD, Bunka DHJ, Forzan M, Spear PG, Stockley PG, Mcgowan I, James W (2011)
603 Generation of neutralizing aptamers against herpes simplex virus type 2: Potential components
604 of multivalent microbicides. *J. Gen. Virol.;* **92:** 1493-1499

605 15. Carfí A, Willis SH, Whitbeck JC, Krummenacher C, Cohen GH, Eisenberg RJ, Wiley DC (2001)
606 Herpes simplex virus glycoprotein D bound to the human receptor HveA. *Mol. Cell;* **8:** 169-179

607 16. Yang D, Meng X, Yu Q, Xu L, Long Y, Liu B, Fang X, Zhu H (2013) Inhibition of hepatitis C virus
608 infection by DNA aptamer against envelope protein. *Antimicrob. Agents Chemother.;* **57:** 4937-
609 4944

610 17. Woo H-, Kim K-, Lee J-, Shim H-, Cho S-, Lee W-, Ko HW, Keum Y-, Kim S-, Pathinayake P, Kim
611 C-, Jeong Y- (2013) Single-stranded DNA aptamer that specifically binds to the influenza virus
612 NS1 protein suppresses interferon antagonism. *Antiviral Res.;* **100:** 337-345

613 18. Wang Y, Li Z, Weber TJ, Hu D, Lin C-, Li J, Lin Y (2013) In situ live cell sensing of multiple
614 nucleotides exploiting DNA/RNA aptamers and graphene oxide nanosheets. *Anal. Chem.;* **85:**
615 6775-6782

616 19. McKeague M, Velu R, Hill K, Bardóczy V, Mészáros T, DeRosa MC (2014) Selection and
617 characterization of a novel DNA aptamer for label-free fluorescence biosensing of ochratoxin A.
618 *Toxins;* **6:** 2435-2452

619 20. Pertel PE, Fridberg A, Parish ML, Spear PG (2001) Cell Fusion Induced by Herpes Simplex
620 Virus Glycoproteins gB, gD, and gH-gL Requires a gD Receptor but Not Necessarily Heparan
621 Sulfate. *Virology;* **279:** 313-324

622 21. Tiwari V, Darmani NA, Thrush GR, Shukla D (2009) An unusual dependence of human
623 herpesvirus-8 glycoproteins-induced cell-to-cell fusion on heparan sulfate. *Biochem. Biophys.*
624 *Res. Commun.;* **390:** 382-387

625 22. Antoine TE, Mishra YK, Trigilio J, Tiwari V, Adelung R, Shukla D (2012) Prophylactic,
626 therapeutic and neutralizing effects of zinc oxide tetrapod structures against herpes simplex
627 virus type-2 infection. *Antiviral Res.;* **96:** 363-375

628 23. Alekseev O, Tran AH, Azizkhan-Clifford J (2012) Ex vivo organotypic corneal model of acute
629 epithelial herpes simplex virus type I infection. *J Vis Exp;*

630 24. Thakkar N, Jaishankar D, Agelidis A, Yadavalli T, Mangano K, Patel S, Zeynep Tekin S, Shukla
631 D (2017) Cultured corneas show dendritic spread and restrict herpes simplex virus infection
632 that is not observed with cultured corneal cells. *Sci. Rep.;* **7:** 42559

633 25. Burnett JC, Rossi JJ (2012) RNA-based therapeutics: Current progress and future prospects.
634 *Chem. Biol.;* **19:** 60-71

635 26. Peacock H, Bachu R, Beal PA (2011) Covalent stabilization of a small molecule-RNA complex.
636 *Bioorg. Med. Chem. Lett.;* **21:** 5002-5005

637 27. Patil SD, Rhodes DG, Burgess DJ (2005) DNA-based therapeutics and DNA delivery systems:
638 A comprehensive review. *AAPS Journal;* **7:**

639 28. McKeague M, Derosa MC (2012) Challenges and opportunities for small molecule aptamer
640 development. *J. Nucleic Acids;* **2012:**

641 29. Hianik T, Ostatná V, Sonlajtnerova M, Grman I (2007) Influence of ionic strength, pH and
642 aptamer configuration for binding affinity to thrombin. *Bioelectrochemistry;* **70:** 127-133

643 30. Hadigal SR, Agelidis AM, Karasneh GA, Antoine TE, Yakoub AM, Ramani VC, Djalilian AR,
644 Sanderson RD, Shukla D (2015) Heparanase is a host enzyme required for herpes simplex virus-1
645 release from cells. *Nat. Commun.;* **6:**

646 31. Agelidis AM, Hadigal SR, Jaishankar D, Shukla D (2017) Viral Activation of Heparanase Drives
647 Pathogenesis of Herpes Simplex Virus-1. *Cell Rep.;* **20:** 439-450

648 32. Antoine TE, Hadigal SR, Yakoub AM, Mishra YK, Bhattacharya P, Haddad C, Valyi-Nagy T,
649 Adelung R, Prabhakar BS, Shukla D (2016) Intravaginal zinc oxide tetrapod nanoparticles as
650 novel immunoprotective agents against genital herpes. *J. Immunol.;* **196:** 4566-4575

651 33. Jaishankar D, Buhrman JS, Valyi-Nagy T, Gemeinhart RA, Shukla D (2016) Extended release
652 of an anti–heparan sulfate peptide from a contact lens suppresses corneal herpes simplex virus-
653 1 infection. *Invest. Ophthalmol. Vis. Sci.;* **57:** 169-180

654

655

656

Target	Direction	Sequence
GAPDH	**Forward**	CAC CAC CAA CTG CTT AGC AC
	Reverse	CCC TGT TGC TGT AGC CAA AT
IFN-α	**Forward**	GAT GGC AAC CAG TTC CAG AAG
	Reverse	AAA GAG GTT GAA GAT CTG CTG GAT
IFN-β	**Forward**	CTC CAC TAC AGC TCT TTC CAT
	Reverse	GTC AAA GTT CAT CCT GTC CTT
TNF-α	**Forward**	AGC CCA TGT TGT AGC AAA CCC
	Reverse	GGA CCT GGG AGT AGA TGA GGT
IL-1β	**Forward**	TCG CCA GTG AAA TGA TGG CT
	Reverse	TGG AAG GAG CAC TTC ATC TGT T
gD	**Forward**	TAC AAC CTG ACC ATC GCT TC
	Reverse	GCC CCC AGA GAC TTG TTG TA

657 **Table 1**: The list of primers used for amplifying cDNA transcripts of RNA extracted from HCE

658 cells.

659

660

GAPDH	**Forward**	CCT GCT GGC TGT GAG GAA AT
	Reverse	GAC AGG GCT CTC CAG ACT TC
IFN-α	**Forward**	CCT GCT GGC TGT GAG GAA AT
	Reverse	GAC AGG GCT CTC CAG ACT TC
IFN-β	**Forward**	TGT CCT CAA CTG CTC TCC AC
	Reverse	CAT CCA GGC GTA GCT GTT GT
IL-1β	**Forward**	GTG GCT GTG GAG AAG CTG TG
	Reverse	GAA GGT CCA CGG GAA AGA CAC

661 **Table 2**: The list of primers used for amplifying cDNA transcripts of RNA extracted from mouse
662 tissue.

663

664 Figures

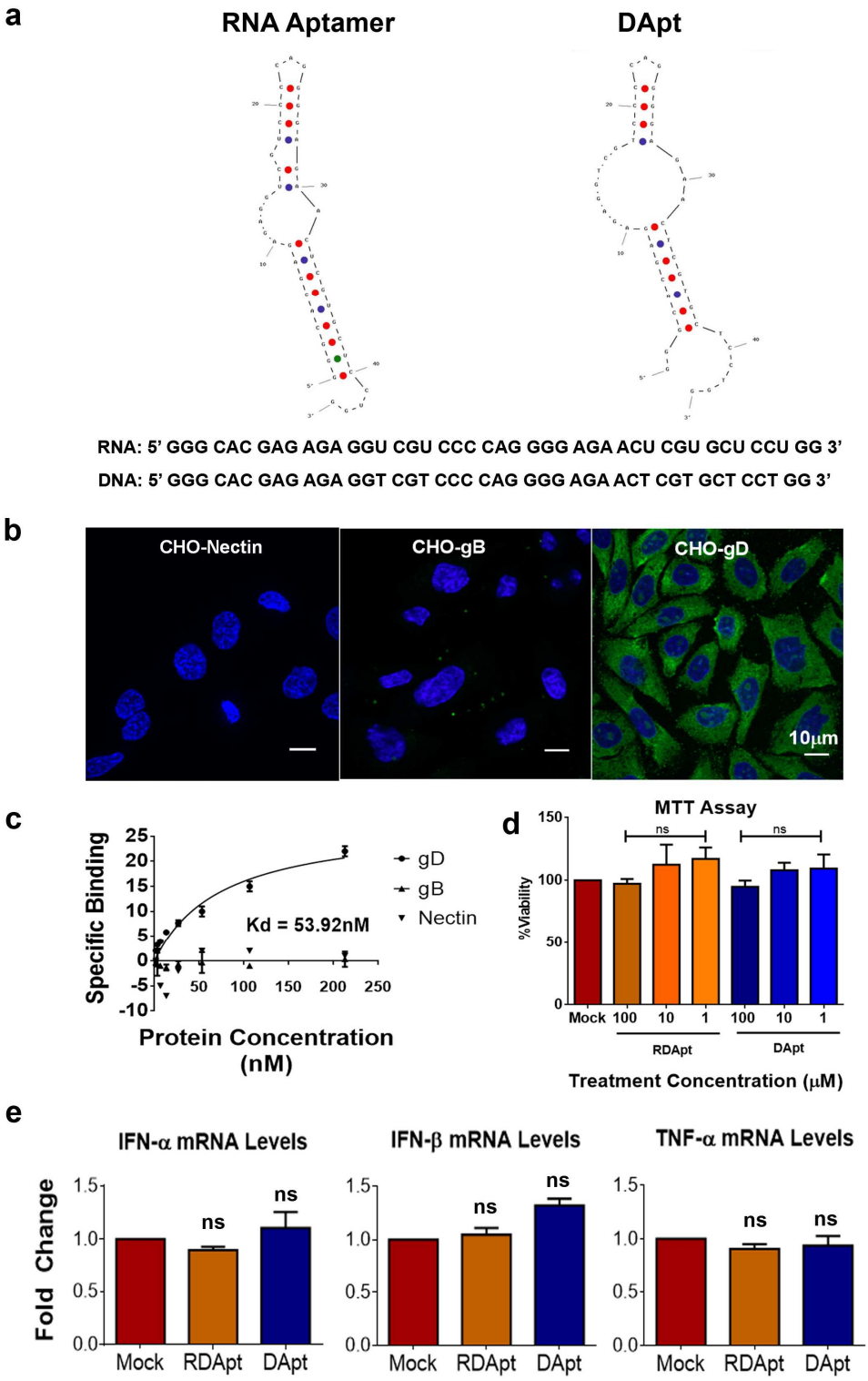

665

666 **Figure 1: Physio-chemical and biological properties of the Aptamer. (a)** The functional
667 sequence of the RNA aptamer with preserved gD protein binding affinity is shown along with
668 the DNA aptamer that was designed from the same. Both aptamers have a similar structure as
669 evaluated by OligoAnalyzer tool available from IDT. **(b)** Representative confocal images of CHO
670 cells expressing either Nectin (left), HSV-1 gB (middle) or HSV-1 gD (right) viral glycoprotein and
671 incubated with FAM modified DApt (GFP). CHO-cells were transfected using lipofectamine
672 protocol with host protein Nectin-1, viral glycoprotein gB or viral glycoprotein gD for 24 hours.
673 The cells were then fixed and permeabilized before they were incubated with FAM-tagged DApt
674 (GFP) for 30 minutes to initiate attachment between DApt and target proteins. Scale bar is
675 same for all images. **(c)** Binding affinity was determined using a modified SYBR green assay.
676 Varying concentrations of protein (Nectin, gB or gD) were incubated with DApt in a 96 well
677 plate for a period of 30 minutes before SYBR green was added to each well. Unbound DApt
678 would sequester SYBR green to produce fluorescence, which was recorded using a fluorescence
679 spectrometer. Change in fluorescence was used as an estimate to calculate specific binding of
680 DApt to mentioned proteins. The Specific binding affinity constant (Kd) shown on the graph was
681 calculated using standardized non-linear regression analysis using GraphPad-Prism software for
682 the interaction between DApt and gD protein. **(d)** Aptamer toxicity was assessed using an MTT
683 assay on HCEs that were incubated with indicated concentrations of PBS, DApt and RDApt for a
684 period of 24h. Data are represented as means ± SD. The values have been normalized to mock
685 treated samples. **(e)** Pro-inflammatory cytokine analysis via qRT-PCR on HCEs incubated with 2
686 µM of indicated treatments for 24h. Data are represented as means ± SD. Data points were
687 normalized to GAPDH. One-way ANOVA with Dunnett's multiple comparison test with a single
688 pooled variance: $p<0.0001$.

689

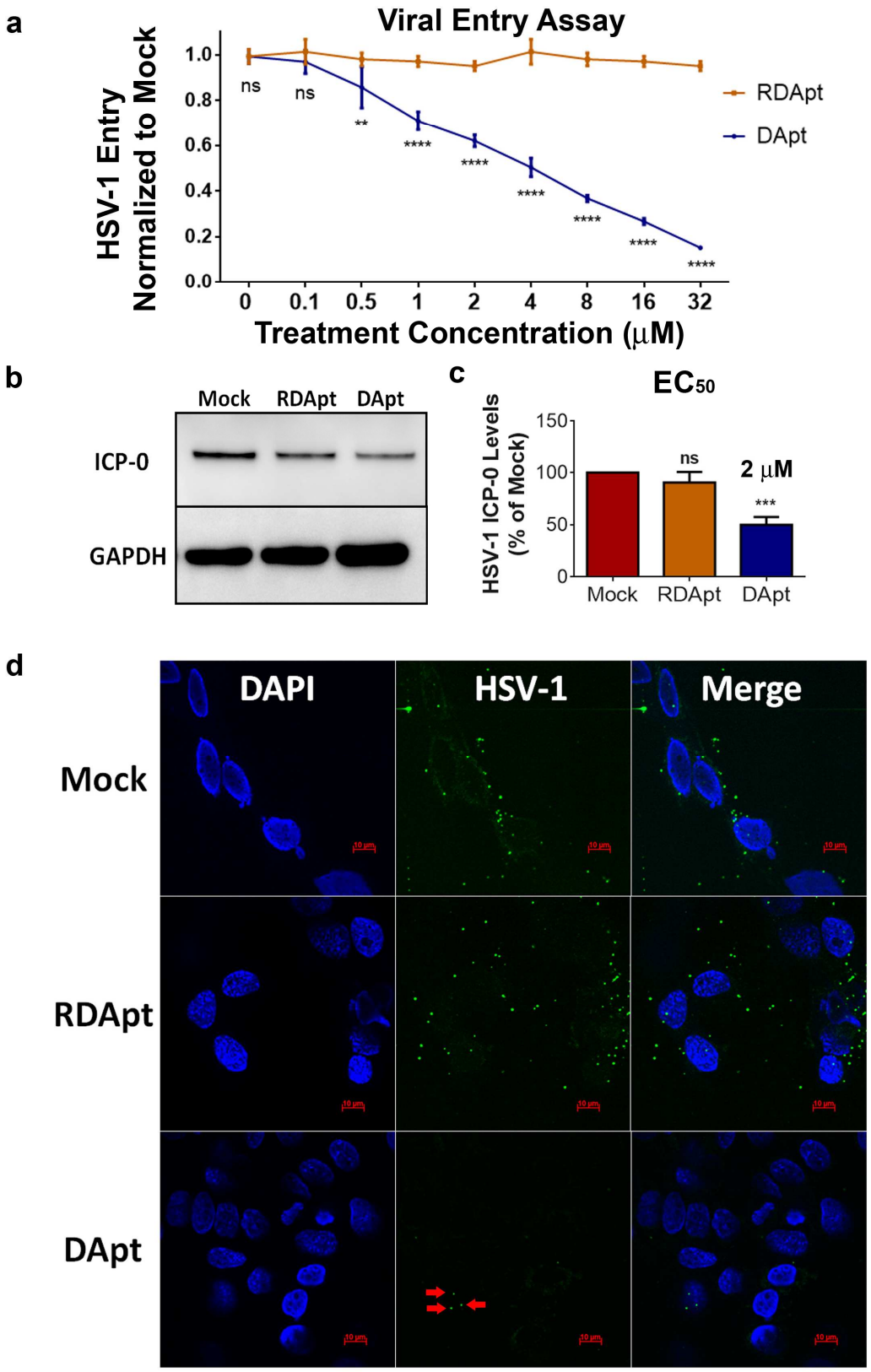
a
Viral Entry Assay
HSV-1 Entry Normalized to Mock
1.0
0.8
0.6
0.4
0.2
0.0
ns
ns
**
****
****
****
****
****
****
0
0.1
0.5
1
2
4
8
16
32
Treatment Concentration (μM)
RDApt
DApt
b
Mock
RDApt
DApt
ICP-0
GAPDH
c
EC50
HSV-1 ICP-0 Levels (% of Mock)
150
100
50
0
ns
2 μM
***
Mock
RDApt
DApt
d
DAPI
HSV-1
Merge
Mock
RDApt
DApt

690

691 **Figure 2: DApt restricts HSV-1 Entry. (a)** HSV-1 viral entry into HCEs was assessed using a β-
692 galactosidase-expressing reporter virus. MOI 10 HSV-1 gL86 was neutralized with the
693 DApt/RDApt at the indicated concentrations for 30 minutes before infecting the cells. *Asterisks*
694 indicate significant difference by Two-way ANOVA with Sidak's multiple comparison test:
695 **p<0.01 and ****p<0.0001. **(b-c)** Representative immunoblots (b) and quantification (c) of
696 HSV-1 ICP-0 (early) protein levels at 6 hpi in HCEs infected with MOI 10 HSV-1(KOS). The virus
697 was neutralized with 2 µM (EC-50) Mock/DApt/RDApt for 30 minutes prior to infection.
698 *Asterisks* indicate significant difference by one-way ANOVA with Dunnett's multiple comparison
699 test with a single pooled variance: ***p<0.0003 **(d)** Representative confocal images of HCE cells
700 showing the presence of internalized GFP virus in HCEs. HSV-1(17-GFP) at MOI 10 were
701 incubated with either 2 µM Mock (PBS)/RDApt/DApt for 30 minutes at room temperature prior
702 to infecting the cells at 4 ^{o}C for 2h. Viral entry was initiated by placing the cells at 37 ^{o}C for 30
703 minutes before cells were fixed and imaged. Scale bar for all images: 10 µm.

704

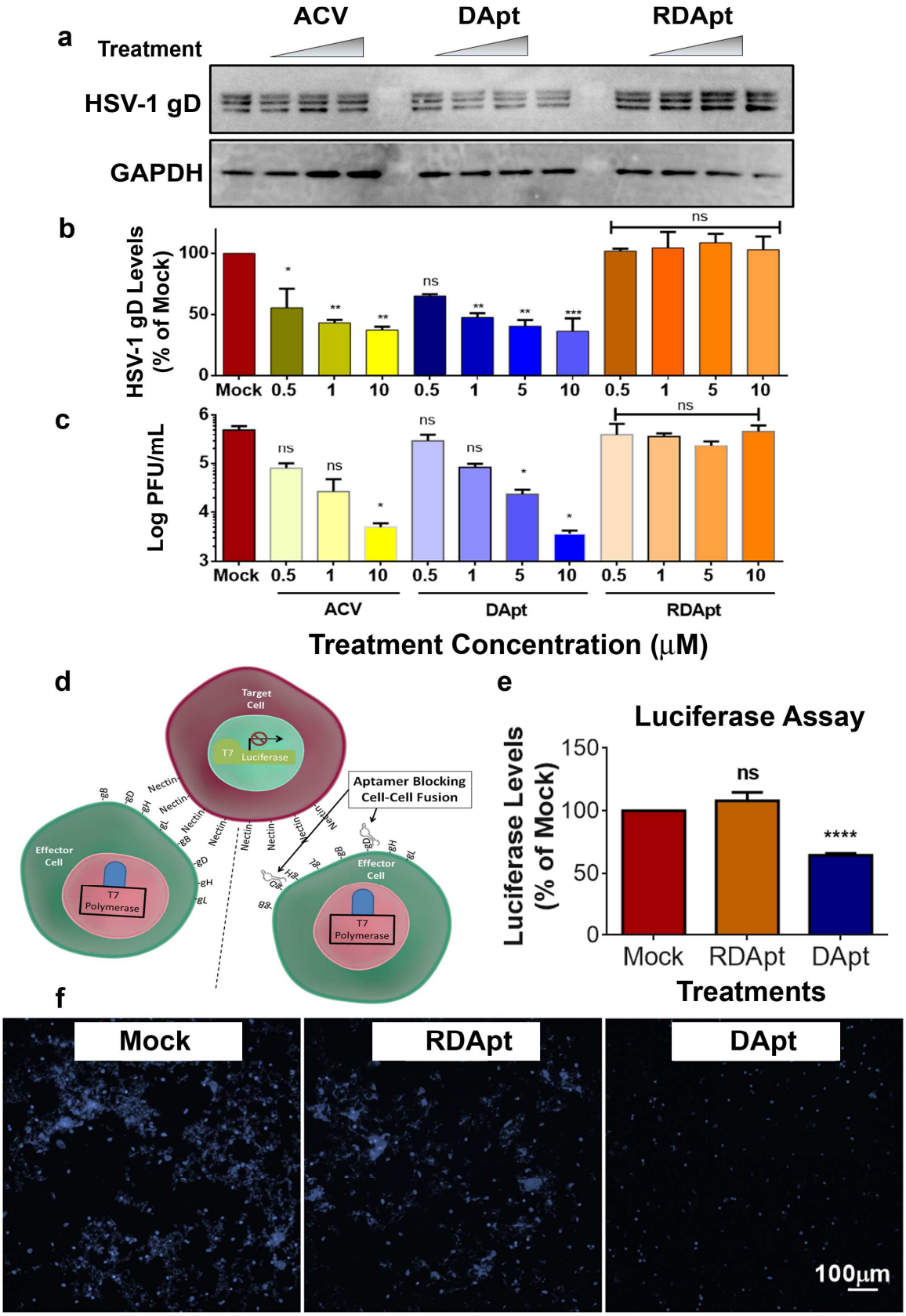
a
Treatment
ACV
DApt
RDApt
HSV-1 gD
GAPDH
b
HSV-1 gD Levels (% of Mock)
100
50
0
Mock 0.5 1 10 0.5 1 5 10 0.5 1 5 10
ns
c
Log PFU/mL
6
5
4
3
Mock 0.5 1 10 0.5 1 5 10 0.5 1 5 10
ACV
DApt
RDApt
Treatment Concentration (μM)
d
Target Cell
T7
Luciferase
Aptamer Blocking Cell-Cell Fusion
Effector Cell
T7 Polymerase
Nectin
e
Luciferase Assay
Luciferase Levels (% of Mock)
150
100
50
0
ns
****
Mock
RDApt
DApt
Treatments
f
Mock
RDApt
DApt
100μm

705

706 **Figure 3: DApt reduces viral replication and minimizes cell to cell spread**. **(a)** Representative
707 immunoblots, **(b)** quantification of HSV-1 gD protein levels **(c)** and supernatant Plaque assays at
708 24 hpi in HCEs infected with HSV-1(KOS) at MOI 1. The virus was neutralized with indicated
709 concentrations of Mock(PBS)/ACV/DApt/RDApt for a period of 30 minutes prior to infection.
710 *Asterisks* indicate significant difference by one-way ANOVA with Dunnett's multiple comparison
711 test with a single pooled variance: *p<0.05, **p<0.01 and ***p<0.001. **(d).** Schematic of cell to
712 cell fusion assay. CHO cells were categorized into two populations: effector (green) and target
713 (red) cells. Effector cells express HSV-1 glycoproteins (gD, gB, gH, gL) and T7 polymerase, while
714 the target cells express nectin-1 (a gD receptor) and the luciferase gene under T7 promoter.
715 Luciferase activity was detected when the cells fuse. **(e)** Luciferase values representing fusion of
716 CHO cells. Effector CHO cells were treated with either 2 µM Mock (PBS)/DApt/RDApt for 30
717 minutes before they were mixed with target CHO cells. *Asterisks* indicate significant difference
718 by one-way ANOVA with Dunnett's multiple comparison test with a single pooled variance:
719 ****p<0.0001. **(f)** Representative fluorescence microscopy images of fused CHO cells showing
720 the presence of syncytial cluster formation (in blue). Effector CHO cells were pre-treated with 2
721 µM Mock (PBS)/DApt/RDApt for 30 minutes before they were added to the target CHO cells.
722 Images of the syncytial cluster were taken by dyeing the cells with NucBlue™ live cell nucleus
723 stain. Scale bar is similar for all images.

724

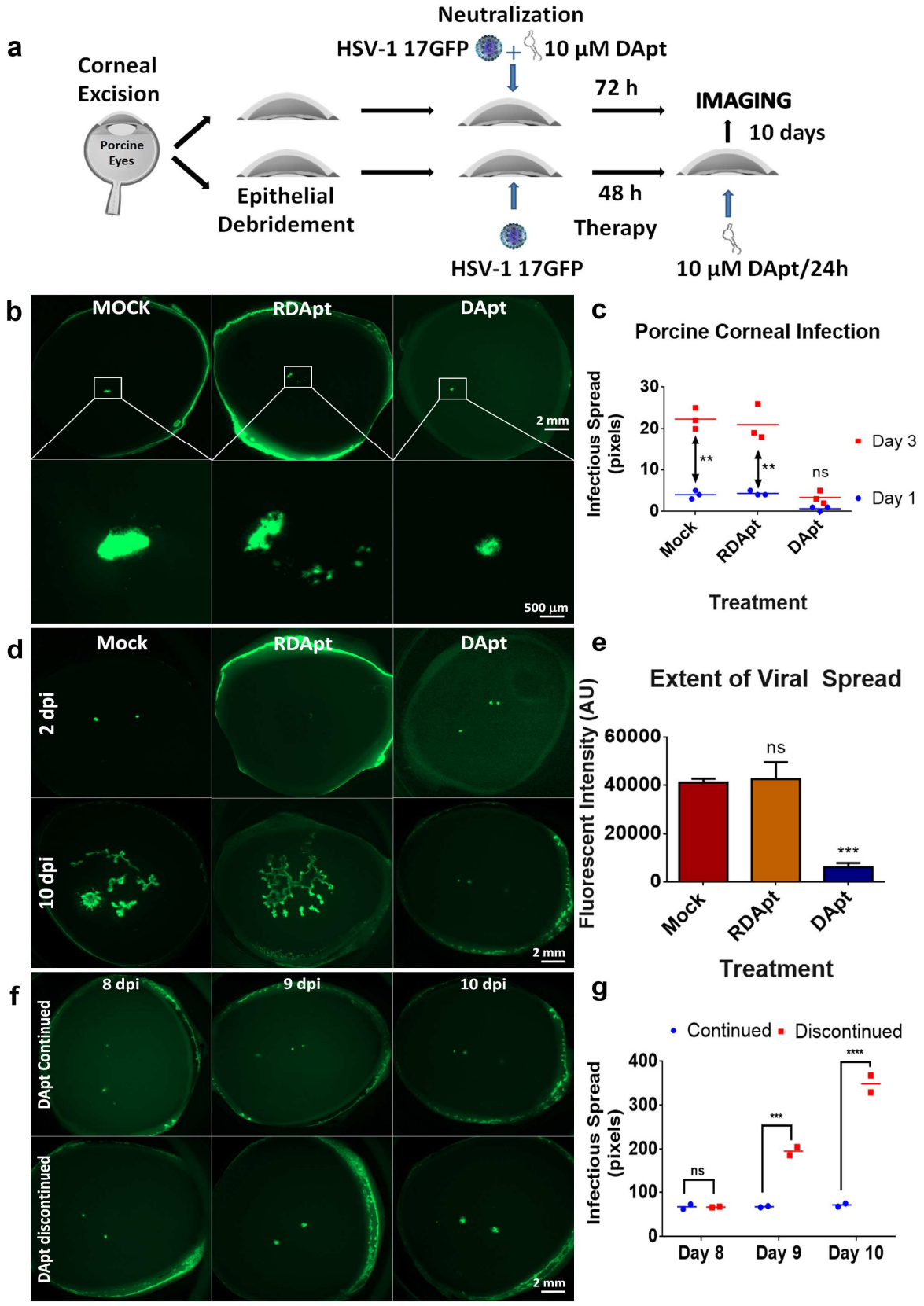
a
Corneal Excision
Porcine Eyes
Epithelial Debridement
Neutralization
HSV-1 17GFP
10 µM DApt
72 h
48 h
Therapy
HSV-1 17GFP
IMAGING
10 days
10 µM DApt/24h
b
MOCK
RDApt
DApt
2 mm
500 µm
c
Porcine Corneal Infection
Infectious Spread (pixels)
Day 3
Day 1
Mock
RDApt
DApt
Treatment
d
Mock
RDApt
DApt
2 dpi
10 dpi
2 mm
e
Extent of Viral Spread
Fluorescent Intensity (AU)
ns
***
Mock
RDApt
DApt
Treatment
f
8 dpi
9 dpi
10 dpi
DApt Continued
DApt discontinued
2 mm
g
Continued
Discontinued
Infectious Spread (pixels)
ns
***
****
Day 8
Day 9
Day 10

725

726 **Figure 4: DApt reduces HSV-1 infection in the *ex vivo* models**. **(a)** A schematic of the *ex vivo*
727 model. Porcine corneas were excised and poked (at the centre of the cornea) with a 30G needle
728 to cause epithelial debridement. Following this, the porcine corneas were infected and treated
729 by DApt to check for its neutralization capabilities or therapeutic efficacy. **(b)** Representative
730 porcine corneal images showing the presence of virus (green) at 72 hpi. The figures shown on
731 the top half were imaged at 7.5 x magnification while the bottom half are the magnified images
732 of the same corneas at 32X. $1x10^6$ PFU HSV-1(17-GFP) was neutralized with 10 µM Mock
733 (PBS)/DApt/RDApt for 30 minutes prior to infecting the porcine corneas. The corneas were
734 washed with PBS and media was replenished every 24 h for 3 days. No additional treatments
735 were added during this period. **(c)** Quantification of viral spread from the poke site. The plot
736 represents difference in areal spread of infection in individual corneas neutralized by indicated
737 treatments over a 3 day period. *Asterisks* indicate significant difference by Repeated measures
738 Two-way ANOVA with Sidak's multiple comparison test: **p<0.01. **(d)** Representative porcine
739 corneal images showing the presence of virus (green) at indicated times. Porcine corneas were
740 infected with 10^6 PFU HSV-1(17-GFP) for 48 h to initiate infection. Therapeutic treatment was
741 started at 48 hpi by addition of 10 µM Mock (PBS)/DApt/RDApt. The corneas were washed and
742 treatments were then added every 24h for 10 days. **(e)** Quantification of viral spread from the 2
743 poke-sites. The plot represents difference in fluorescence intensity (virus spread) between
744 corneas treated by indicated treatments for a period of 10 days. *Asterisks* indicate significant
745 difference by One-way ANOVA with Dunnett's multiple comparison test with a single pooled
746 variance: ***p<0.001. **(f)** Representative porcine corneal images showing the presence of virus
747 (green) at indicated times. Within the therapeutic model, at 7 dpi, DApt treatment was
748 continued on one set of porcine corneas while the other set was left untreated for 72 h in order
749 to evaluate changes in infectious spread. Scale bars shown are same for all the images. **(g)**
750 Representative fluorescence intensity values for corneas which continued to receive DApt
751 treatment or for which DApt treatment was discontinued.

752

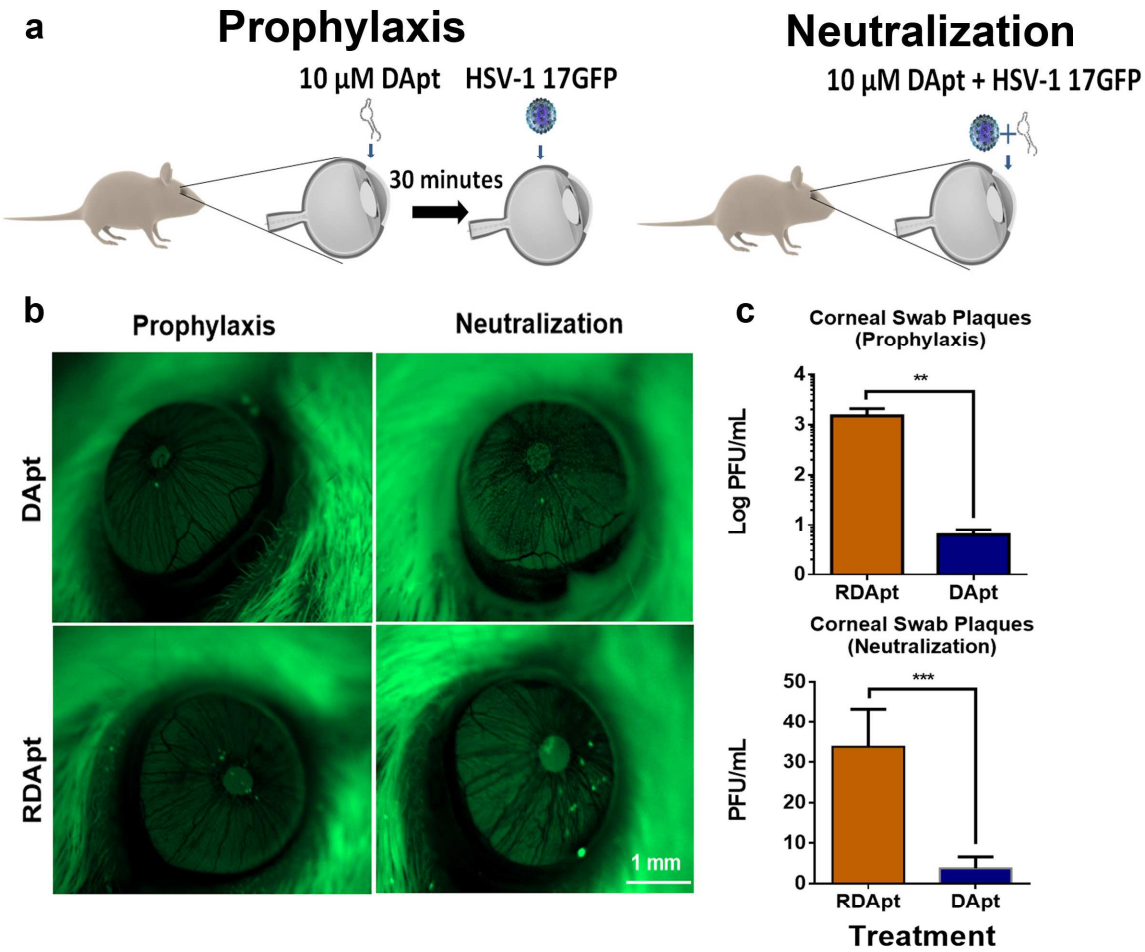
a
Prophylaxis
10 µM DApt
HSV-1 17GFP
30 minutes
Neutralization
10 µM DApt + HSV-1 17GFP
b
Prophylaxis
Neutralization
DApt
RDApt
1 mm
c
Corneal Swab Plaques (Prophylaxis)
Log PFU/mL
**
RDApt
DApt
Corneal Swab Plaques (Neutralization)
PFU/mL
***
RDApt
DApt
Treatment

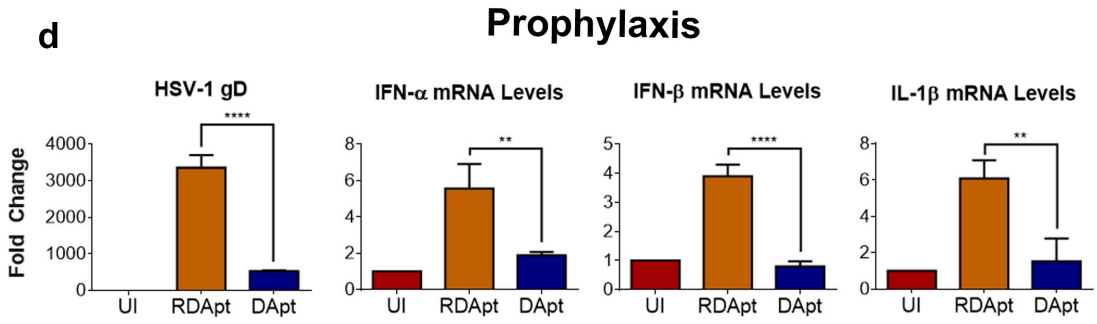
d
Prophylaxis
HSV-1 gD
IFN-α mRNA Levels
IFN-β mRNA Levels
IL-1β mRNA Levels
Fold Change
****
**
****
**
UI
RDApt
DApt

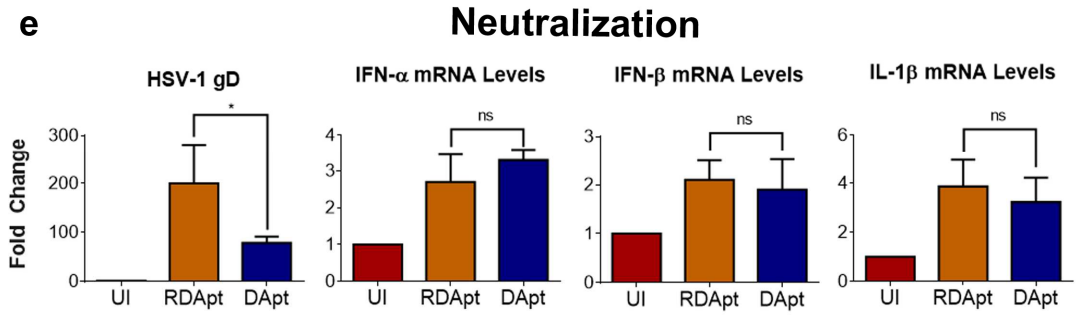
e
Neutralization
HSV-1 gD
IFN-α mRNA Levels
IFN-β mRNA Levels
IL-1β mRNA Levels
Fold Change
*
ns
ns
ns
UI
RDApt
DApt

753

754 **Figure 5: Prophylaxis and Neutralization treatments of DApt inhibit HSV-1 infection in the *in***
755 ***vivo* model. (a)** A schematic of the prophylactic and neutralization treatments conducted on
756 the mouse corneal models. Mice were sedated and the corneal epithelium was partially
757 debrided using a 30G needle. For the prophylactic model, corneas were treated with 10 µM
758 DApt/RDApt for 30 minutes before infecting with 10^6 PFU HSV-1 (17-GFP). For the
759 neutralization model, 10^6 PFU HSV-1 (17-GFP) were incubated with 10 µM DApt/RDApt for 30
760 minutes and then added to the corneas. **(b)** Representative stereoscope images of the mouse
761 cornea taken 48 hpi for the indicated treatments showing the presence of virus (green). Scale
762 bars shown are for all the images. **(c)** Tears of the infected mice, in the form of corneal swabs,
763 were collected 72 hpi and a plaque assay was conducted with the same to understand the
764 extent of infection in each mice. Plaque numbers for each treatment group are shown. *Asterisks*
765 indicate significant difference by Unpaired t-tests: **p<0.0021 (Prophylaxis), ***p<0.0009
766 (Neutralization) **(d-e)** Fold change in IFN-α, IFN-β and IL-1β transcript levels in enucleated
767 mouse eyes quantified via qRT-PCR. Mouse corneal tissue was harvested 72 hpi. *Asterisks*
768 indicate significant difference by One-way ANOVA with Dunnett's multiple comparison test with
769 a single pooled variance: *p<0.05, **p<0.01, ***p<0.001 and ****p<0.0001.

770

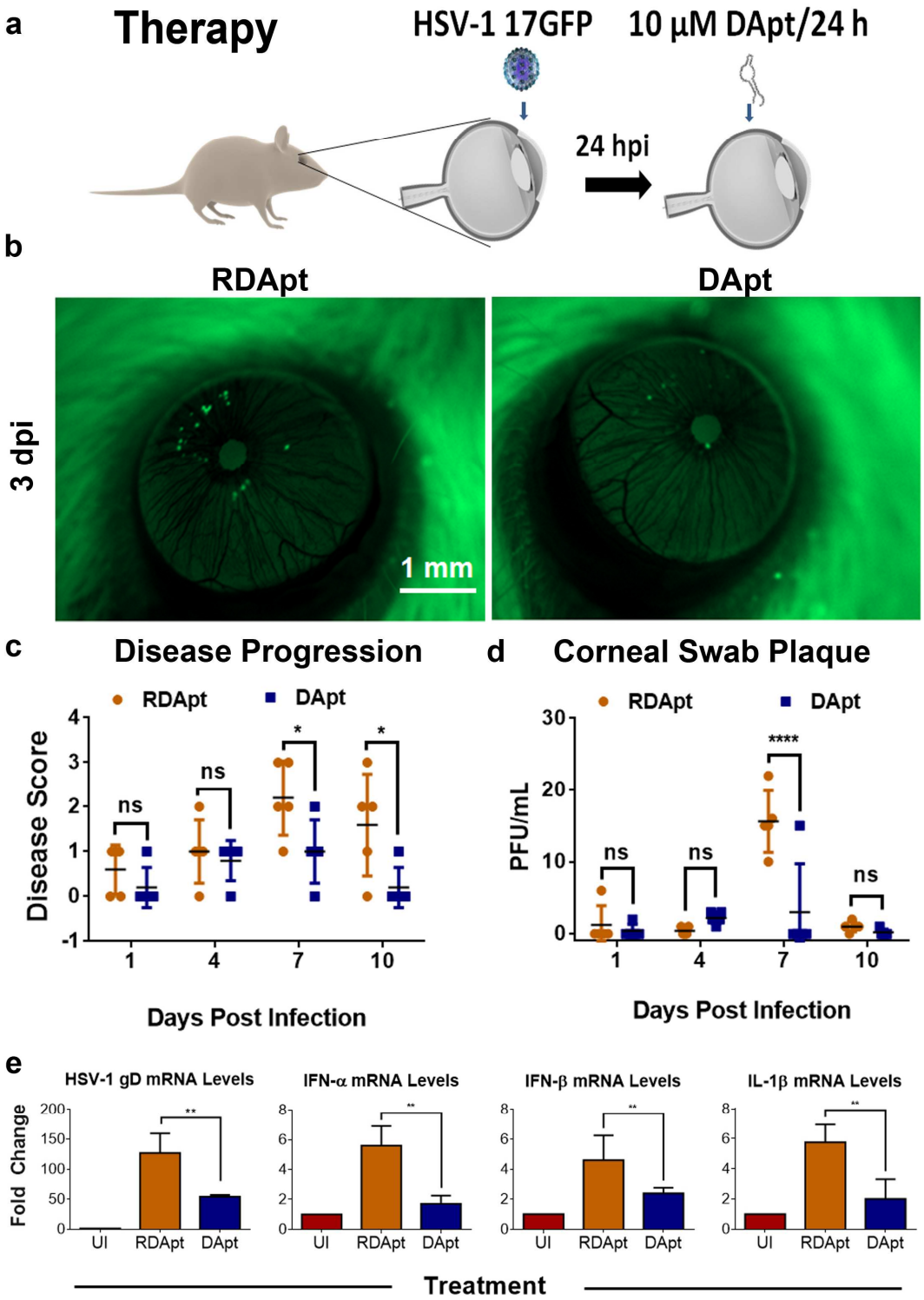
a
Therapy
HSV-1 17GFP
10 µM DApt/24 h
24 hpi
b
RDApt
DApt
3 dpi
1 mm
c
Disease Progression
RDApt
DApt
Disease Score
ns
ns
*
*
Days Post Infection
d
Corneal Swab Plaque
RDApt
DApt
PFU/mL
ns
ns
****
ns
Days Post Infection
e
HSV-1 gD mRNA Levels
IFN-α mRNA Levels
IFN-β mRNA Levels
IL-1β mRNA Levels
Fold Change
UI
RDApt
DApt
Treatment

771

772 **Figure 6: Therapeutic treatment of DApt inhibits HSV-1 infection in the *in vivo* model. (a)** A
773 schematic of the therapeutic treatment conducted on the mouse corneal models. Mice were
774 sedated and the corneal epithelium was partially debrided using a 30G needle prior to infection
775 with 10^7 PFU of HSV-1(17-GFP). 24 hpi, the mice were given a dose of either 10 µM DApt or
776 RDApt followed by a dose every 24 h till 72 hpi. **(b)** Representative stereoscope images taken at
777 indicated times to show presence of virus (green). Scale bars shown are for all the images. **(c)**
778 Animals were scored based on disease progression following HSV-1 (17-GFP) infection for a
779 period of 14 days as follows: 0, no lesions; 1, minimal eyelid swelling; 2, moderate swelling; 3,
780 moderate swelling with ocular discharge; 4, eyelid swelling with corneal opacity; 5, severe
781 swelling of the eyelid with hair loss and dendritic lesions. *Asterisks* indicate significant
782 difference by Two-way ANOVA with Sidak's multiple comparison test: *$p<0.05$ **(d)** Tears of the
783 infected mice, in the form of corneal swabs, were collected at indicated times and a plaque
784 assay was conducted with the same to understand the extent of infection in each mice. Plaque
785 numbers for each treatment group are shown. *Asterisks* indicate significant difference by Two-
786 way ANOVA with Sidak's multiple comparison tests: ****$p<0.0001$ **(e)** Fold change in IFN-α,
787 IFN-β and IL-1β transcript levels in enucleated mouse eyes quantified via qRT-PCR. Mouse
788 corneal tissue was harvested 72 hpi. *Asterisks* indicate significant difference by One-way
789 ANOVA with Dunnett's multiple comparison test with a single pooled variance: **$p<0.01$ and
790 ***$p<0.001$.

791

792 Supplementary Files

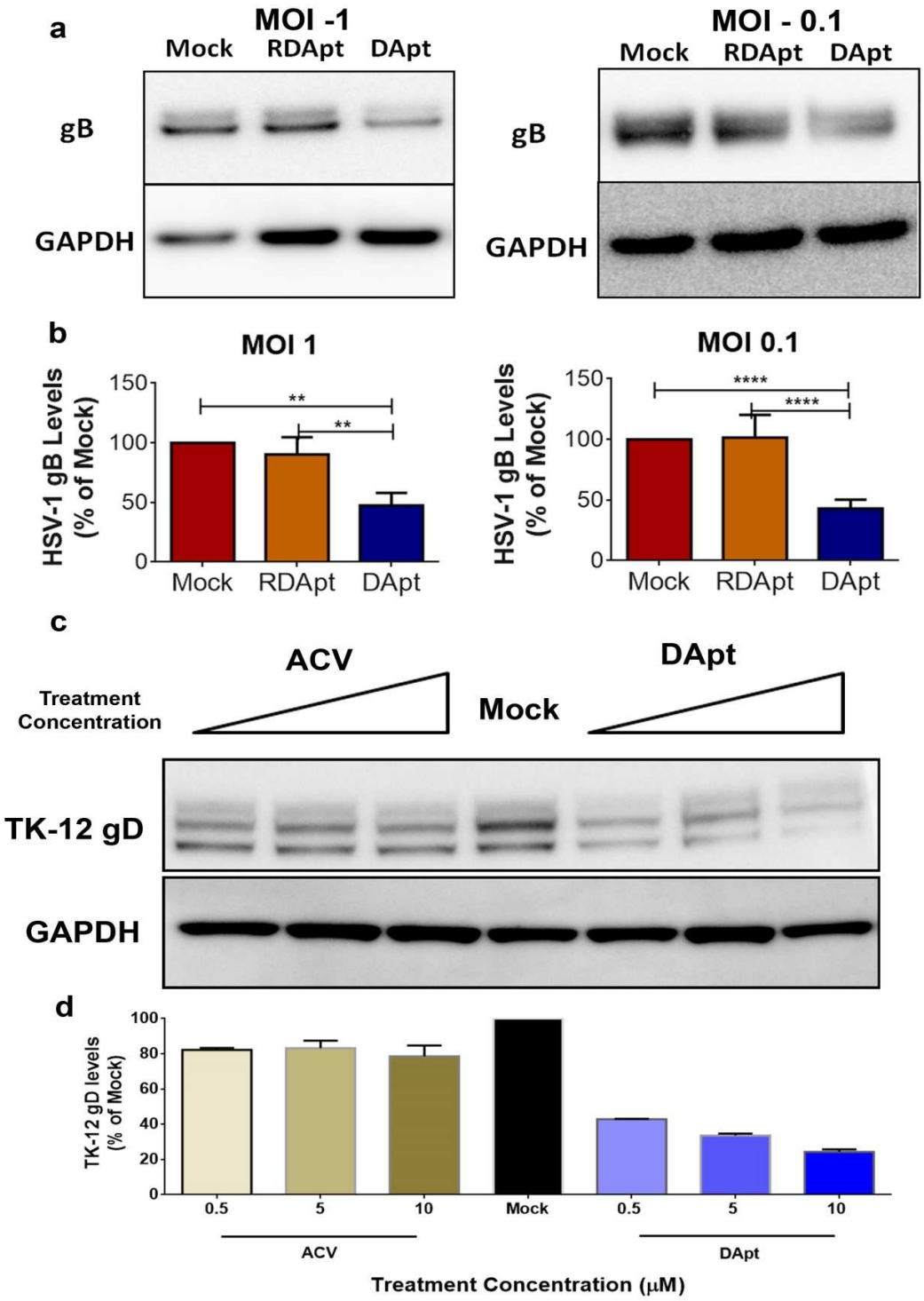

793

794 **Supplementary figure S1: DApt neutralizes acyclovir resistant virus. (a)** HSV-1 (KOS) at MOI 1
795 and 0.1 were neutralized with 2 µM DApt/RDApt for a period of 30 minutes before they were
796 allowed to infect HCEs. At 2 hpi, cell monolayer was washed with PBS twice and fresh MEM
797 media was added. 24 hpi, cells were collected, lysed and immunoblotted for HSV-1 gB to
798 evaluate effective infectious levels. **(b)** The immunoblots were analyzed and quantified using
799 image J software. **(c)** HSV-1 (TK-12) virus which is HSV-1 Thymidine Kinase null (molecular target
800 for acyclovir) was neutralized with Acyclovir/Mock/DAPt at indicated concentrations for a
801 period of 30 minutes before they were allowed to infect monolayer of HCE cells. At 2 hpi, cells
802 were washed with PBS twice and fresh MEM media was added. 24 hpi, cells were lysed and
803 immunoblotted for the presence of HSV-1 gD. **(d)** Immunoblots were quantified and analyzed
804 using Image J software and plotted using GraphPad Prism software.

805

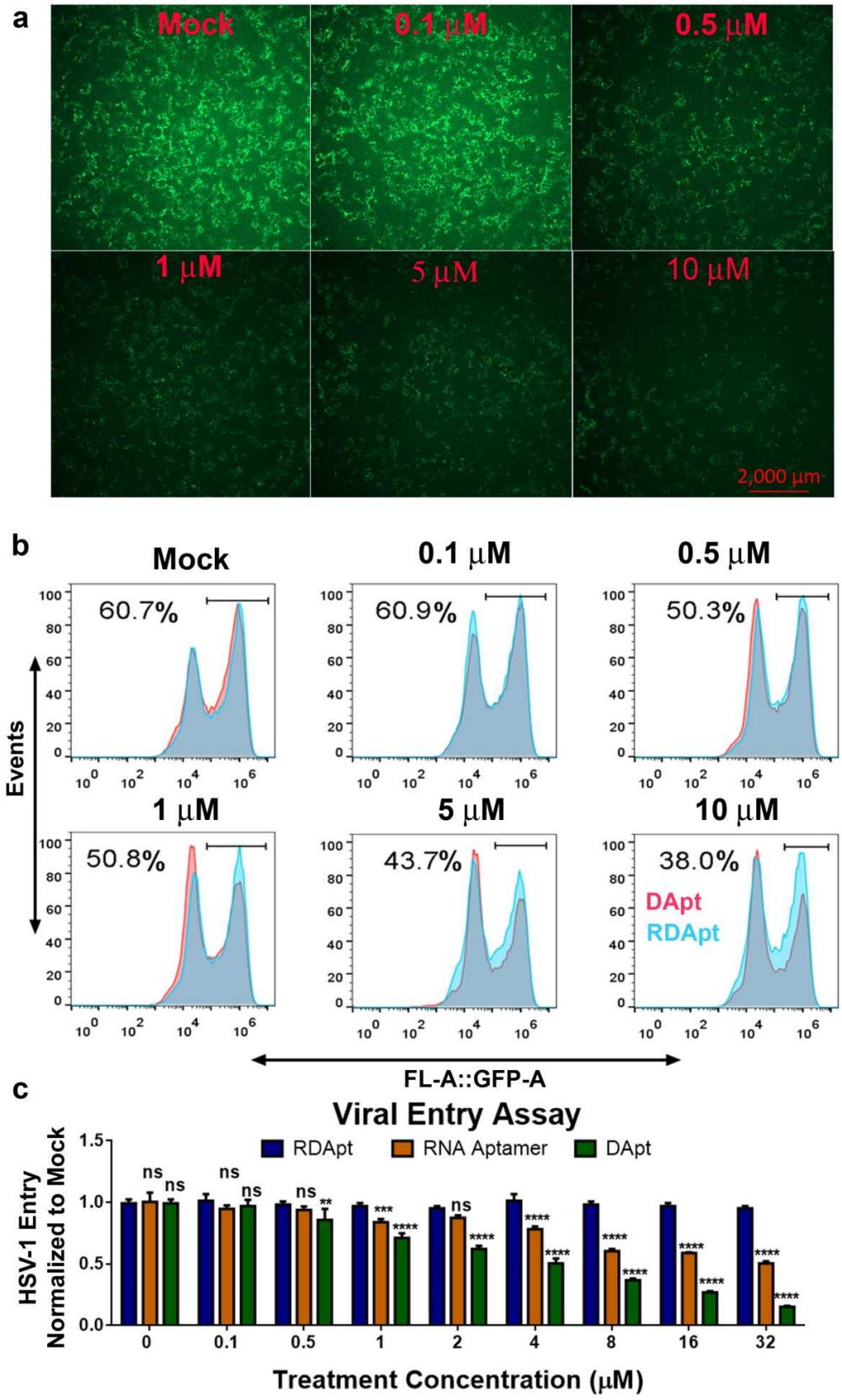
a
Mock
0.1 μM
0.5 μM
1 μM
5 μM
10 μM
2,000 μm
b
Mock
0.1 μM
0.5 μM
1 μM
5 μM
10 μM
60.7%
60.9%
50.3%
50.8%
43.7%
38.0%
DApt
RDApt
Events
FL-A::GFP-A
c
Viral Entry Assay
RDApt
RNA Aptamer
DApt
HSV-1 Entry Normalized to Mock
Treatment Concentration (μM)

806

807 **Supplementary Figure S2. DApt neutralizes HSV-1 virus in-vitro. (a)** HSV-1 (17-GFP) was
808 neutralized with increasing concentrations of DApt/RDApt for a period of 30 minutes before
809 they were allowed to infect HCE cells for 2 hours in a 24 well plate. At 2 hpi, cells were washed
810 with PBS twice and fresh MEM media was added. At 24 hpi, cells were washed with PBS and
811 imaged using Zeiss Stereoscope (7x magnification; 400 ms exposure) in the GFP channel. **(b)**
812 Cells were then trypsinized, collected and washed with FACS buffer (2% fetal bovine serum in
813 PBS) and filtered through a 63 micron nylon filter to remove any aggregates from the sample.
814 300 µL samples were analyzed using a BD Accuri C6 Plus Flow cytometer at 25,000 gated events
815 for singlet cells. The data was analyzed using FloJo software. **(c)** Viral Entry assay was
816 performed using HSV-1 gL 86 β-galactosidase producing reported virus, neutralized either by
817 pre-heated (90 °C) and cooled RNA Aptamer (dissolved in 50 mM Tris-HCl, 50 mM KCl [pH 7.5]),
818 DApt or RDApt (dissolved PBS) at indicated concentrations for 30 minutes. Neutralized virus
819 was added to HCEs plated in a 96 well plate and incubated for 6 hours before the cells were
820 lysed and suitable substrate (0.5% Nonidet P40 and 3 mg/mL ONPG, o-nitro-phenyl- β-d-
821 galactopyranoside; ImmunoPure, PIERCE, Rockford, IL) solution was added to each well. The
822 plates were stored at 37 °C for a period of 2 hours before the enzymatic activity was analyzed
823 using a GENESIS Pro Plate reader at 410 nm. *Asterisks* indicate significant difference by two-way
824 ANOVA with Sidak's multiple comparison test: **$p<0.01$, ***$p<0.001$ and ****$p<0.0001$

825

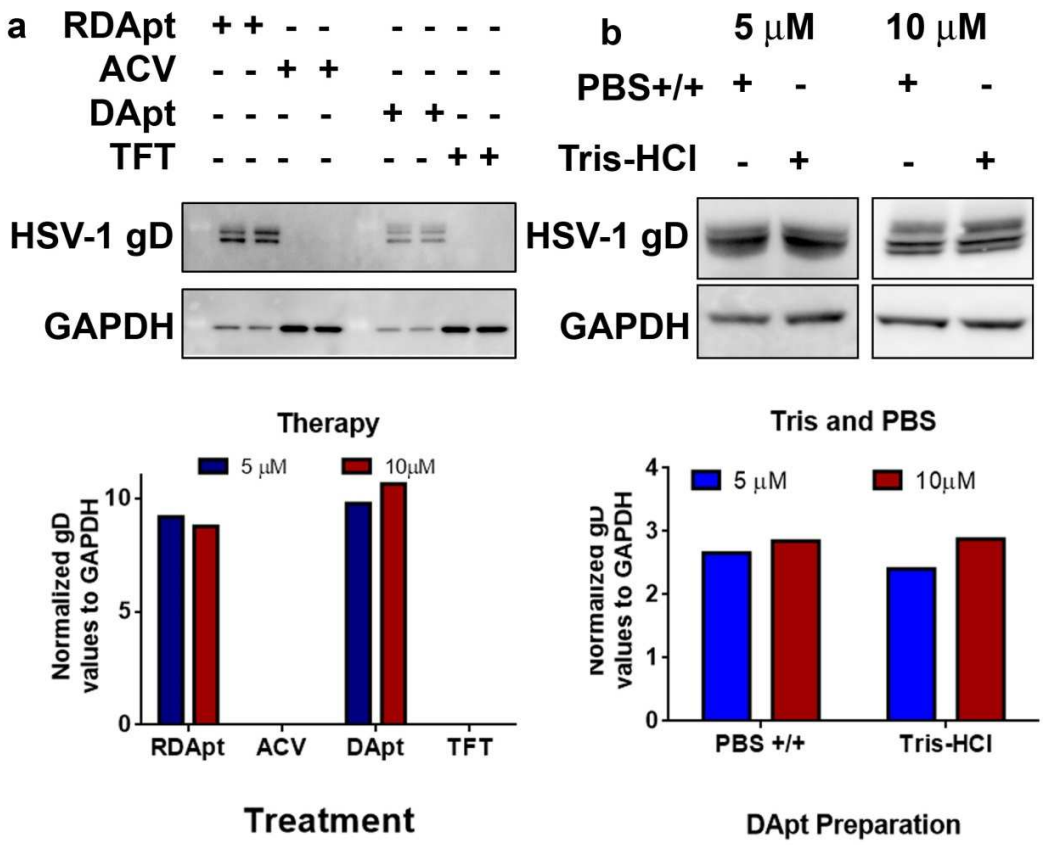

Supplementary Figure S3. DApt shows minimal therapeutic efficacy *in vitro*. (a) HSV-1 (KOS) at MOI 1 was used to infect HCE cells. At 2 hpi, cells were washed with PBS twice and MEM media with indicated concentrations of either RDApt/ACV/DApt/TfT was added to the cell monolayer. The treatments were incubated with the cells overnight and at 24 hpi, cells were lysed and immunoblotted for the presence of HSV-1 gD protein. The blots were analyzed using Image J software and the quantifications are shown. **(b)** To understand the difference in neutralizing ability of the DApt while dissolved in different buffers, indicated concentrations of DApt/RDApt were dissolved in Tris buffer (50 mM Tris-HCl, 50 mM KCl [pH 7.5]) or PBS +/+ (gibco, Life Technologies; $CaCl_2$ and $MgCl_2$ [pH 7.0]). Pre-heated and cooled aptamers were used to neutralize HSV-1 (KOS) at MOI 1 for 30 minutes before infecting HCE cells. At 2 hpi, cells were washed with PBS twice and fresh MEM media was added. At 24 hpi, cells were lysed and immunoblotted for HSV-1 gD. The blots were analyzed using Image J software and the quantifications are shown.